

Classification-based Machine Learning Approaches to Predict the Taste of Molecules: A Review

Cristian Rojas^{a,*}, Davide Ballabio^b, Viviana Consonni^b, Diego Suárez-Estrella^a, Roberto Todeschini^b

^a Grupo de Investigación en Quimiometría y QSAR, Facultad de Ciencia y Tecnología, Universidad del Azuay, Av. 24 de Mayo 7-77 y Hernán Malo, Cuenca 010107, Ecuador

^b Milano Chemometrics and QSAR Research Group. Department of Earth and Environmental Sciences, University of Milano-Bicocca, P.za della Scienza 1-20126, Milano, Italy

*Corresponding author. E-mail: crojasvilla@gmail.com

Abstract

The capacity to discriminate safe from dangerous compounds has played an important role in the evolution of species, including human beings. Highly evolved senses such as taste receptors allow humans to navigate and survive in the environment through information that arrives to the brain through electrical pulses. Specifically, taste receptors provide multiple bits of information about the substances that are introduced orally. These substances could be pleasant or not according to the taste responses that they trigger. Tastes have been classified into basic (sweet, bitter, umami, sour and salty) or non-basic (astringent, chilling, cooling, heating, pungent), while some compounds are considered as multitastes, taste modifiers or tasteless. Classification-based machine learning approaches are useful tools to develop predictive mathematical relationships in such a way as to predict the taste class of new molecules based on their chemical structure. This work reviews the history of multicriteria quantitative structure-taste relationship modelling, starting from the first ligand-based (LB) classifiers proposed in 1980 by Lemont B. Kier and concluding with the most recent studies published in 2022.

Keywords

Taste chemistry; Machine learning; Taste classification; QSAR models; Foodinformatics

1. Background

30 **1.1. Taste chemistry**

31 **1.1.1. Introduction**

32 Considering the incredible variability of environmental conditions on the planet, the availability of
33 specific foods has played a key role in the adaptive evolution and conservation of species. Indeed, the
34 availability of specific types of nutrition may be one of the most important variables in the evolution
35 of species. Taste and olfaction are the two senses that allow the discrimination of chemical substances
36 (Schieberle & Hofmann, 2016). Dangerous tastes have been empirically correlated with bitterness;
37 however, some of the most ancient medicines include bitter substances (Bayer *et al.*, 2021). Recently,
38 scientific approaches have been replacing empiric ways to understand and to assess the safety of food
39 products. While these scientific approaches have been shown to be useful in the analysis and
40 categorizing of tastes, some foods that are considered safe may illicit, intolerances and allergies in a
41 few people. For instance, human intolerances to gluten and lactose are well known, along with the
42 life threatening anaphylactic allergic response to seafood and peanuts. These relatively rare reactions
43 to food are related to specific digestive enzymes concentrations, and to the human immune system,
44 respectively.

45 Beyond safety considerations, each person has specific preferences for tastes that can change over
46 one's lifetime. This variation in personal taste preferences could be related to biochemical, as well as
47 environmental, psychological and cultural factors. This diversity of factors makes it difficult to
48 describe the taste mechanisms, e.g. psychologists might consider taste preferences to be related
49 mainly to psychological stimulus, while chemists might think that tastes are perceived primarily
50 through the consequence of chemical reactions that occur in tissues (Behrens & Ziegler, 2020),
51 contributing to kind and intensity of sensations. In this framework, the identification of the healthiest,
52 safest and most preferred foods is of fundamental importance to the food and pharmaceutical
53 industries. Research related to the mechanisms underlying the human perception of tastes is
54 increasing in the last few years (Damodaran & Parkin, 2017). Importantly, current research into tastes
55 and sensory perceptions are being studied from different, but related and interconnected directions,
56 such as chemical, biochemical, anatomical, physiological, and psychological standpoints.

57 It is common to identify "tastes" or "flavors" as the combination of taste, olfactory, tactile and thermal
58 sensations (Di Lorenzo *et al.*, 2009), while sensomics is the mapping of the combinatorial code of
59 aroma and taste by active key molecules. These molecules are sensed by human chemosensory
60 receptors (Schieberle & Hofmann, 2016). The extraordinary developments in foodinformatics
61 (computational food chemistry) and bioinformatics (computational biochemistry) are providing new

62 tools to assess and to explain the receptor/ligand binding affinity and how the structures of the
63 receptors interact with the chemical structures of the compounds and how to achieve a particular taste
64 of interest (Martinez-Mayorga & Medina-Franco, 2014; Rojas *et al.*, 2016a). At the beginning of
65 sensory research, the greatest efforts were focused on the chemical structure of compounds, their
66 characteristics and the cultural particularities of populations. It was considered that chemical analysis
67 of taste molecules in raw ingredients and in end-products for human consumption could play an
68 important role for the assurance of food quality and desirability preventing defects in products (Ley
69 *et al.*, 2012). However, this approach was not sufficient to explain all the taste phenomena. Later, the
70 importance of the complex anatomy and physiology of taste receptors and how they interact with
71 specific tastant molecules were recognized as key factors to better understand and model the
72 phenomenon of taste.

73 A molecular tastant is considered to be a water-soluble chemical able to produce taste sensations by
74 activating taste receptor cells (TRCs) and thus activate taste-related pathways at within the nervous
75 system (Di Lorenzo *et al.*, 2009; Rojas *et al.*, 2022). Tastants are elicited not only in water, but also
76 in organic and inorganic acids and amino acids, all of which are able to facilitate the interactions of
77 tastants with receptors (Chaudhari *et al.*, 2009). Chemosensory receptors located in the taste buds of
78 the tongue are fundamental to the regulation of taste sensation. Other mechanisms to recognize
79 molecular tastants are, for example, the opening of ion channels or through secondary messenger
80 channels associated with nucleotides or phosphorylated inositol (Damodaran & Parkin, 2017; Morini
81 *et al.*, 2011; Wong, 2018).

82 Taste measurement is preferably performed by an experienced panel of assessors. Panelists are trained
83 with standard solutions of the basic tastes by means of the sip and spit methodology (Kelly *et al.*,
84 2005; Spillane *et al.*, 2006). The concentrations of standard solutions should be prepared at a
85 minimum of their recognition threshold to ensure taste detection (Deng *et al.*, 2021; Liu *et al.*, 2020;
86 Shiyan *et al.*, 2021; Spillane *et al.*, 2006; Yu *et al.*, 2018). The pH of the standard solutions also
87 influences taste perception. Then, a solution of an unknown analyte (generally at concentration of 0.01
88 M) is provided to members of the panel who are asked to identify the basic taste and aftertaste. The
89 taste potency of the unknown analyte can be estimated by the amount that the solution should be
90 diluted to be equal to the standard. The evolution of technology led to the development of some
91 analytical procedures based on sensors for the sensory evaluation of foods; for instance, electronic
92 noses and tongues, in which their operation is based on the measurement of potential differences that
93 are related to the tastes and aromas that humans can sense (Deng *et al.*, 2021; Liang *et al.*, 2022a;
94 Suárez-Estrella *et al.*, 2021; Xiu *et al.*, 2022).

95 **1.1.2. Basic tastes**

96 Currently, five basic tastes have been identified: sweet, bitter, umami, sour and salty, which are
97 referred to as basic taste modalities, taste qualities or receptor-mediated tastes (Chandrashekar *et al.*,
98 2006; Damodaran & Parkin, 2017; Di Lorenzo *et al.*, 2009; Morini *et al.*, 2011; Wong, 2018). Among
99 the basic tastes, sweetness is probably the most important one, since sweeteners evoke a high caloric
100 intake and a pleasant sensation in many foods and medicines (Chandrashekar *et al.*, 2006; Damodaran
101 & Parkin, 2017). Most sweet foods contain mono- and disaccharides (Di Lorenzo *et al.*, 2009), which
102 are responsible for their sweetness and quick sources of energy for the body. On the other hand,
103 several non-caloric substances capable of providing a sensation of sweetness to food are currently
104 known and are used in the industry. Those substances may have both natural or artificial origins
105 (Chattopadhyay *et al.*, 2014).

106 Sweetness perception is related to the presence of a glycochore unit in the sweetener's scaffold. It
107 forms the tripartite model (AH, B and γ units), which interacts with the sweetness receptor along a
108 multipoint attachment (MPA) construct. The sweet taste chemoreceptor is a G-protein coupled
109 receptor (GPCR) of class C composed of the T1R2 (Type 1 Receptor 2) and T1R3 (Type 1 Receptor
110 3) subunits, which are composed of three structural domains (Chandrashekar *et al.*, 2006; Morini *et al.*,
111 2011; Wong, 2018). The presence of the AH-B sites in a tastant molecule is a necessary, but not
112 a sufficient condition alone to elicit sweetness; for example, the sweetness taste can be viewed as a
113 function of the size, shape and functionality of the compounds (Spillane & Sheahan, 1989). In other
114 words, a large molecule must be able to fit specifically into the receptor site to generate sweetness. A
115 small molecule with the AH-B site might be unable to match the construct of the receptor site, and
116 the sweet stimulus may not be produced.

117 Sucrose has a clean (no aftertastes) sweet sensation (even at high concentrations), and consequently
118 it is frequently used as the standard to quantify the relative sweetness (RS) or sweetness potency (Sw)
119 of sweet-tasting molecules (Liu *et al.*, 2020; Rojas *et al.*, 2022; Shiyan *et al.*, 2021; Yu *et al.*, 2018).
120 Sweet potency is defined as the concentration ratio between a sucrose solution standard labeled as 1
121 (or 100%), and the solution of a sweetener exhibiting the same intensity (iso-sweet concentration)
122 (Rojas *et al.*, 2016a; Rojas *et al.*, 2016b). Sweeteners could be classified as natural (nutritive or
123 carbohydrate) and artificial (non-nutritive or non-carbohydrate) (Ley *et al.*, 2012; Wong, 2018; Yang
124 *et al.*, 2022). On the other hand, certain amino acids and proteins are detected as sweet compounds
125 and some salts taste sweet at low concentrations, including NaCl, KCl, NaOH, KOH, salts of
126 beryllium and lead acetate and carbonate (Di Lorenzo *et al.*, 2009).

127 Bitterness has been defined as an unpleasant taste. The unpleasant sensation is related to a rejection
128 of some foods, many of which are toxic compounds for humans (Chandrashekar *et al.*, 2006; Di

129 Lorenzo *et al.*, 2009). Thus, bitter perception might be related to an evolved “alert” system to prevent
130 the intake of high concentration of toxic compounds through food or drink, avoiding their undesirable
131 and potential lethal effects (Ley *et al.*, 2012). On the other hand, not all bitter compounds are toxic
132 and not all toxic compounds are bitter. In fact, some of them have proven beneficial effects for human
133 health, for instance, polyphenols, glucosinolates and terpenes (Bayer *et al.*, 2021). Moreover, some
134 bitter tastes may be perceived as pleasant (Dagan-Wiener *et al.*, 2019) as well as associated food
135 products, such as coffee, beer, olives, and unsweetened chocolate. Plants that are perceived as slightly
136 bitter are commonly used for food, while plants perceived as highly bitter are more commonly used
137 in medicines. Plants perceived as having intermediate bitterness might be used for both alimentation
138 and/or medical purposes (Pieroni *et al.*, 2007; Pieroni *et al.*, 2002).

139 Bitter molecules generally require the presence of a polar (electrophilic or nucleophilic) group and a
140 hydrophobic group to interact with the bitter receptor. Bitter taste stimuli are associated with 25
141 receptors (TAS2Rs), which are G protein-coupled (Adler *et al.*, 2000; Chandrashekar *et al.*, 2006;
142 Matsunami *et al.*, 2000). Most of them are located in the same taste receptor cells (TRCs)
143 (Chandrashekar *et al.*, 2006; Damodaran & Parkin, 2017; Di Lorenzo *et al.*, 2009; Wong, 2018).
144 TAS2Rs have not only been identified in the mouth cavity, but also in gastrointestinal, respiratory,
145 reproductive and urinary tract tissues (Bayer *et al.*, 2021). The physiological function of TAS2Rs
146 outside the oral cavity have not been identified. Bitter receptors can be specific for one or a few
147 compounds, while others are able to react to a large number of bitter substances (Di Pizio & Niv,
148 2015). Some bitter compounds are agonists for some TAS2R subtypes, but antagonists for others
149 (Brockhoff *et al.*, 2011). Bitterness is a common taste reaction to alkaloids and heavy metal salts.
150 Quinine sulfate is the standard used for comparisons among the bitterness of compounds (Dagan-
151 Wiener *et al.*, 2017; Damodaran & Parkin, 2017). Quinine sulfate (Liu *et al.*, 2020; Rojas *et al.*, 2022)
152 and L-isoleucine (Shiyan *et al.*, 2021; Yu *et al.*, 2018) are the most frequently used standards for
153 bitterness identification. Quinine is an alkaloid used in the food industry as a component of some soft
154 drinks to infuse them with bitter taste, for example, tonic water. Substances used as sweeteners, such
155 as sodium saccharine and acesulfame K can become bitter at high concentration and also produce a
156 bitter aftertaste (Di Lorenzo *et al.*, 2009).

157 Umami is the most recently recognized basic taste. Umami is a Japanese word that means
158 deliciousness. This taste is associated with L-amino acids (such as monosodium glutamate MSG),
159 that are umami enhancers (potentiators) (Baines & Brown, 2016; Damodaran & Parkin, 2017; Suess
160 *et al.*, 2015; Wong, 2018). For instance, MSG exhibits a synergistic effect (enhancement) with the
161 guanosine 5'-monophosphate or inosine 5'-monophosphate nucleotides, although these compounds
162 also show a weak intrinsic umami taste on their own (Ley *et al.*, 2012; Wong, 2018). Also, L-aspartate

163 produces an umami sensation. Umami taste is detected in meats, cheeses, some mushrooms along
164 with fish, kelp and tomatoes. The umami taste stimuli of peptides and their molecular interactions is
165 associated with G-protein coupled receptors (GPCRs) comprised of the subunits T1R1 (Type 1
166 Receptor 1) and T1R3 (Type 1 Receptor 3) (Liang *et al.*, 2022a; Liang *et al.*, 2022b; Morini *et al.*,
167 2011). An umami nucleotide binds with the corresponding receptor at three points: two of them are
168 electrophilic (A and B) that interact with the two phosphoryl oxygens and the C6 oxygen,
169 respectively, while site X interacts with the substituent at C2, particularly when the substituent is
170 delocalized (Wong, 2018). The standard used to quantify umami intensity is MSG (Baines & Brown,
171 2016; Liu *et al.*, 2020; Rojas *et al.*, 2022; Shiyan *et al.*, 2021; Yu *et al.*, 2018).

172 Sour taste is associated with the presence of organic and inorganic acids in food. Acidity in raw food
173 tends to change with time; for example, acidity in soft fruit decrease as the fruit becomes ripe. A sour
174 taste is associated with unripe soft fruit. Sourness increases also after fermentation processes applied
175 for the production of foods, such as yogurt, wine, vinegar and bread. Initially, sourness perception
176 was related to the capacity of substances to release hydrogen ions in water. However, hydrogen ion
177 release is not the mechanism that produces sourness for organic and diluted inorganic acids (Breslin
178 & Huang, 2006; Roper, 2007). Other mechanisms include proton exchange, a stimulus-gated Ca^{++}
179 channel and the direct entry through an H^+ channel that has not been identified (Di Lorenzo *et al.*,
180 2009). A sour taste can also be induced by the passage of electric current through the tongue that
181 probably generates hydrogen ions from the hydrolysis of acid or water (Damodaran & Parkin, 2017;
182 Wong, 2018). In addition, undissociated acids play an important role in sour perception. For instance,
183 some weak organic acids that naturally occur in foods, such as citric, succinic, malic, or lactic acid,
184 are perceived to be more sour than hydrochloric acid at the same pH (Ley *et al.*, 2012). On the other
185 hand, other acid molecules (i.e., potassium acid oxalate or protocatechuic acid) exhibit both sour and
186 bitter tastes (Wong, 2018). The standard used to assess the sourness in food is citric acid (Liu *et al.*,
187 2020; Rojas *et al.*, 2022; Shiyan *et al.*, 2021; Yu *et al.*, 2018).

188 Saltiness is the sensation produced by some soluble salts, such as those with low molecular-weight,
189 mainly chlorides from sodium, potassium or calcium (Damodaran & Parkin, 2017; Wong, 2018).
190 NaCl is the only compound exhibiting an intense and clean (no after taste) salty taste and it is
191 consequently used as the saltiness standard (Liu *et al.*, 2020; Rojas *et al.*, 2022; Shiyan *et al.*, 2021;
192 Yu *et al.*, 2018). Potassium chloride can be considered a replacement for NaCl, however it can be
193 perceived as a sweet/bitter taste at low concentrations (Di Lorenzo *et al.*, 2009). In contrast, high
194 molecular-weight salts elicit bitter rather than salty taste, such as lithium chloride and ammonium
195 chloride. However, they are limited for human consumption due to safety and their offensive tastes,
196 respectively (Ley *et al.*, 2012; Wong, 2018).

197 The physiological function of the salty taste is to maintain the body's electrolyte balance. In taste
198 buds, ion channels allow the passage of chemical species that trigger stimuli perceived as salty, and
199 there is a relationship between the number of fungiform papillae and sensitivity to salty taste (Doty
200 *et al.*, 2001). Apparently, the salty taste is related to the body's ability to detect sodium, thanks to the
201 specific transduction mechanism of this cation, and its passage through the epithelial-sodium channel
202 (ENaC) in the apical membrane of the receptor cells of taste. The epithelial-sodium channel is the
203 mammalian Na⁺ specific taste receptor. Most mammals have at least one type of salt taste receptor
204 that is cation nonselective, apparently from the salty taste evoked by KCl and NH₄Cl molecules. At
205 the same time, high circulating aldosterone levels suggest aldosterone modulated epithelial cell
206 membrane Na⁺ transporters as candidate for salt taste receptors (DeSimone & Lyall, 2006). Moreover,
207 one or more receptors, such as a variant of TRPV1 (TRPV1t), may be able to respond to various
208 cations including K⁺, Ca²⁺, NH₄⁺ and to Na⁺ (DeSimone & Lyall, 2006; Rhyu *et al.*, 2021).

209 **1.1.3. Non-basic tastes**

210 Some compounds or combinations of compounds can produce tastes considered as non-basic or
211 secondary tastes, such as astringent, chilling, cooling, heating and pungent (Damodaran & Parkin,
212 2017; Ley *et al.*, 2012; Wong, 2018). Moreover, other sensations have also been described as non-
213 basic tastes, such as fattiness, or the definition of water as a tastant. Other characteristics of substances
214 have led to the classifications of compounds as multitastes, taste modifiers or tasteless.

215 The definition of fattiness as a taste has been triggered by the transduction mechanisms that are
216 sensitive to fatty acids in the TRCs membranes (Gilbertson *et al.*, 1997). The transduction
217 mechanisms are associated with the inhibition of delayed rectifying K⁺ channels and through the fatty
218 acid CD36 (Di Lorenzo *et al.*, 2009). Evidence suggests that fatty acids (e.g. linoleic acid, oleic acid
219 and stearic acid) could be considered as tastants and that their tastes are detectable without the need
220 for other sensory cues such as texture, viscosity or smell (Di Lorenzo *et al.*, 2009). On the other hand,
221 water has its own taste, even though it could be affected by temperature and easily affected by diluted
222 compounds even at low concentration. Moreover, it could be considered as a tastant because of the
223 role of water in eliciting compounds in TRCs and in taste nerves of some species (Di Lorenzo *et al.*,
224 2009). It has been suggested that an aquaporin, AQP5, a membrane channel, allows the water
225 molecules to get into the cell by activating and regulating the volume of water through the anion
226 channel (Di Lorenzo *et al.*, 2009). Moreover, when the mouth is rinsed after the application of a sweet
227 taste blocker, water elicited a sweet aftertaste (Di Lorenzo *et al.*, 2009).

228 Multitaste is a complex sensation of tastes elicited by combining more than one basic taste at the
229 same time (Rojas *et al.*, 2022). It is triggered by a variety of different compounds. Some examples of

230 multitaste compounds are the potassium acid oxalate and protocatechuic acid, which produce
231 sour/bitter tastes (Wong, 2018), calcium phenolsulfonate (bitter/astringent tastes) and benzyl acetate
232 (bitter/pungent tastes) (Dagan-Wiener *et al.*, 2019). Some compounds are able to alter and even block
233 the taste of other compounds. Na⁺ channel blockers reduce the saltiness of sodium chloride, thaumatin
234 and adenosine monophosphate block bitterness, while lactisol propionate blocks sweetness. On the
235 other hand, some compounds increase the taste of others (taste enhancers); for example chlorogenic
236 acid and cynarin enhance the sweetness (Di Lorenzo *et al.*, 2009). In contrast, some compounds have
237 antagonist effects, that is, they tend to suppress the taste sensation of other compounds. This is what
238 occurs with citric acid and sucrose tastants in lemonade. It is also possible to find synergistic effects,
239 for instance the enhancement of umami taste by the addition of IMP or GMP to MSG (Di Lorenzo *et*
240 *al.*, 2009).

241 The expression “tastelessness” is used to categorize molecules as lacking any particular taste. These
242 are also classified as non-sweet, non-bitter, non-sour, non-salty or non-umami compounds (Rojas *et*
243 *al.*, 2017; Rojas *et al.*, 2022). Some changes in the chemical structure of substances may modify their
244 sweet taste to a bitter one or make them tasteless. For example, the saccharin sweetener becomes
245 bitter by the introduction of a nitro group onto carbon five (5-nitrosaccharin), while the introduction
246 of this group on the four-carbon position produces a sweet/bitter tastant (*p*-nitrosaccharin). On the
247 other hand, the presence of the amino group produces a sweet/tasteless compound (6-aminosaccharin)
248 or a tasteless molecule (5-aminosaccharin) (refer to Figure 1) (Rojas *et al.*, 2022). Interestingly, some
249 tasteless compounds like miraculin and circulin act as taste modifiers, in particular, these compounds
250 change the sense of sour in substances to sweet. In contrast, gymnemic acid, ziziphin and hodulcin
251 block the sensation of sweetness (Di Lorenzo *et al.*, 2009).

252
253 **Figure 1 should be inserted around here**

254

255 **1.2. Machine learning to uncover Structure-Taste Relationships**

256 Studies of Quantitative Structure-Property Relationships (QSPRs) enhance the definition of
257 mathematical relationships between molecular structures and specific properties of chemical
258 compounds, such as taste. These approaches have played an important role in the evaluation and study
259 how molecular features are related to the taste of chemical substances through the development of
260 empirical data-driven models. QSPR models require molecular descriptors, which are numerical
261 indices that encode the detailed chemical and structural information of molecules. They can be both
262 experimental physicochemical properties of molecules and theoretical indices, which are calculated

263 through mathematical algorithms (Todeschini & Consonni, 2009). Molecular descriptors are used as
264 independent variables in QSPR models. The relationships between descriptors and the property of
265 interest (e.g., the taste of chemicals) are calculated by means of chemometrics and machine learning
266 approaches.

267 The QSPR workflow starts with an appropriate description of the molecular structures and ends with
268 the prediction of the behavior of the chemicals. This approach relies on the assumption that the
269 molecular structure of a substance encodes the chemical features that are responsible for its physical,
270 chemical, and biological behavior. If these features are correctly encoded into numerical descriptors,
271 then QSPR strategy allows first to establish the empirical relationships between descriptors and the
272 property of interest by means of statistical multivariate modeling, and subsequently infers the
273 property of a new substance or untested chemical through the QSPR model.

274 There are several multivariate statistical methods to process molecular descriptors and achieve
275 reliable estimates of chemical properties. Depending on the nature of the modeled property,
276 classification and regression methods can be used to calculate models both for reproducing the known
277 experimental data and predicting the unknown data for qualitative and quantitative responses,
278 respectively. If chemicals belong to defined qualitative classes; for example, molecules labelled as
279 positive or negative, then supervised classification models can be applied. Classification approaches
280 define mathematical relationships between descriptors and classes and can thus be used to predict the
281 class of new substances that are associated with unknown experimental class labels. If chemicals are
282 associated with a quantitative response, regression methods are used to define the mathematical
283 model that relates descriptors and the response to obtain quantitative predictions for new chemicals.

284 The two main operational steps in the development of QSPR models are the definition of their
285 applicability domain and the implementation of proper validation protocols, as proposed by the
286 OECD (Organization for Economic Co-operation and Development) in the framework of the five
287 general principles for QSARs (Gramatica, 2007). These principles are used as the criteria to evaluate
288 and accept QSPRs, especially for regulatory purposes, and state that each model should have: 1) a
289 defined endpoint; 2) an unambiguous algorithm; 3) a defined domain of applicability; 4) appropriate
290 measures of goodness-of-fit, robustness and predictivity; 5) a mechanistic interpretation, if possible.

291 The Applicability Domain (AD) of a QSPR model is the chemical space where predictions can be
292 considered as reliable (Mathea *et al.*, 2016; Sahigara *et al.*, 2012). If the properties of a new untested
293 molecule are predicted through QSPRs, then it is considered to share the same mechanisms and/or
294 modes of action as the molecules used to build the model provided that it is structurally similar to the
295 training molecules and falls inside the AD. In this case, the properties of predicted chemical are
296 considered as interpolated by the model and its predicted properties can be assumed to be reliable. In

297 contrast, the predictions for molecules falling outside the AD can be considered as model
298 extrapolations, and consequently they are considered to be unreliable.

299 Moreover, the attention to effective and reliable estimates through predictive models has a crucial
300 role in the QSPR workflow. When supervised qualitative (classification) or quantitative (regression)
301 approaches are used to establish structure-property relationships, the primary goal of the process is to
302 achieve reliable models that are able to correctly predict the properties of new untested molecules.
303 QSPR modeling could also have explanatory purposes, that is, allowing the interpretation of the
304 relationship between descriptors and the modeled property to deepen the knowledge about the specific
305 problem in analysis. In both cases, validation protocols for the assessment of the predictive ability of
306 models and the reliability of the established relationships should be always applied (Oliveri, 2017;
307 Wold & Eriksson, 1995). This step is necessary also to avoid overfitted models, that is, models in
308 which mathematical relationships accurately predict properties for the training compounds, but not
309 for new untested substances.

310 The predictive abilities of the models are usually evaluated by splitting the available compounds into
311 training and test sets. Training compounds are used to establish the mathematical model, which is
312 then used to predict the responses of the chemicals included in the test set. Finally, the agreement
313 between of experimental and predicted responses for the test substances is evaluated to assess the
314 model's predictive ability. Several validation protocols exist and the usage of a particular one usually
315 depends on how many chemicals are available for model development. A general requirement is that
316 molecules in the test chemical space should be reasonably similar to that of the training space.
317 However, large degrees of similarities could produce an excessively optimistic evaluation of a
318 model's predictive ability. For this reason, when dealing with classification models, it is preferable
319 to keep the class balance equal in the training and test sets; that is, the same distribution of chemicals
320 in the modeled classes should be preserved in both sets.

321 **1.2.1. Classification approaches**

322 In the framework of machine learning applied to QSPR, classification methods are fundamental
323 techniques aimed at finding mathematical relationships that recognize the class membership of
324 molecules on the basis of a set of molecular descriptors. Once a classification model has been trained,
325 the membership of unknown chemicals to one of the defined classes can be predicted. Thus, for
326 discrete molecular properties, like qualitative properties distinguishing between different tastes, a
327 general representation of classification models is the following:

328

$$329 \quad C = f(x_1, x_2, \dots, x_p) \quad (1)$$

330

331 where C is the class, x_1, \dots, x_p are p (number) of molecular descriptors, and f is a function representing
332 the relationship between the class and the descriptors.

333 Several classification methods have been proposed in the last decades, with different characteristics,
334 advantages and limitations (Lavine & Rayens, 2009). A preliminary distinction among classification
335 methods can be defined on the basis of the mathematical form of the decision boundary: linear
336 methods calculate the best linear boundary for class discrimination, while non-linear methods
337 discriminate classes by non-linear boundaries.

338 Another important difference can be made between discriminant (pure classification) and class-
339 modeling methods. Discriminant methods divide the whole chemical space defined by the molecular
340 descriptors in as many regions as the number of the modeled classes. Thus, each compound is
341 assigned the class corresponding to the region of the chemical space where it falls. On the other hand,
342 class-modeling methods (also known as one-class classifiers) define the boundary to separate a
343 specific class from the rest of the chemical space. Thus, a target class is modeled independently of
344 the others; compounds fitting the class model are considered members of the class, while chemicals
345 that are outside the class space are classified as non-members of the target class.

346 Among classification methods, Discriminant Analysis (DA) is the most widely used (Hand, 1997;
347 McLachlan, 1992). DA finds the directions in the multivariate space that maximizes the ratio of the
348 between-class to within-class variances; these are called discriminant functions and from a
349 mathematical point of view, these directions are linear combinations of the original variables.
350 Depending on the choice of the class-covariance representation, two different discriminant methods
351 can be distinguished: Quadratic Discriminant Analysis (QDA) and Linear Discriminant Analysis
352 (LDA), which define quadratic and linear boundaries between classes, respectively. One major
353 drawback for DA is that it cannot be applied to datasets with the number of samples lower than the
354 dimension of the measurement space. However, to overcome this limitation, DA can be combined
355 with methods for dimensionality reduction, such as variable selection approaches or principal
356 component analysis (PCA).

357 Another option to deal with highly dimensional spaces is the application of Partial Least Squares
358 Discriminant Analysis (PLSDA) (Barker & Rayens, 2003; Brereton & Lloyd, 2014). PLSDA benefits
359 from the properties of PLS (Partial Least Squares) regression, since it searches for the latent variables,
360 that is, the directions of maximum covariance with the response to be modeled. The difference from
361 PLS is that the response encodes class membership with binary codes and class thresholds have to be
362 defined to predict samples in one of the modeled classes.

363 Unlike DA and PLSDA, which are discriminant classifiers, the Soft Independent Modeling of Class
364 Analogy (SIMCA) method is one of the most useful and popular class-modeling approaches. It is
365 based on PCA carried out on the samples of the target class. To predict the class of test samples, the
366 sample distances from the class PCA model are calculated on the basis of normalized Q residuals and
367 Hotelling's T^2 values, which measure how well each sample conforms to the model. Only samples
368 with distances lower than a defined threshold are classified into the class space.

369 Another class modeling approach consists of the calculation of Potential Functions (PFs), where the
370 assignment of a new sample to the target class is based on the cumulative potential of the class, which
371 is calculated as the sum of the individual potentials of the target class samples in the point of the
372 chemical space where the new sample is projected. The shape of the potential depends on the choice
373 of the type of potential function (kernel) and smoothing parameter (Brereton, 2011).

374 Tree-based algorithms exploit different classification approaches. They recursively divide data into
375 smaller subgroups, which contain samples belonging to as few classes as possible. In each split, the
376 partition is achieved by maximizing the purity of the new subsets. The final classification model
377 consists of a collection of nodes that define the classification rule. One of the most common tree-
378 based approaches is the Classification and Regression Tree (CART), which selects the variables that
379 provide the purest subsets of samples in each node (Breiman *et al.*, 1984). The Random Forest (RF)
380 method represents a subsequent development of tree-based approaches (Breiman, 2001). It is a meta-
381 classifier based on an ensemble of classification trees, each trained on various subsamples of the
382 training set, which are built by bootstrapping. The prediction is then obtained by majority vote among
383 the classifications provided by the trees of the forest.

384 Another approach, based on the ensemble of models, is AdaBoost (Adaptive Boosting), where
385 predictions provided by many "weak" classifiers are pooled to produce a better classification.
386 Predictions are combined through an adaptive iterative algorithm that exploits the weighted majority
387 voting (Freund & Schapire, 1997). Besides the original boosting method, other approaches have been
388 proposed and applied for the prediction of molecular taste, especially when dealing with big datasets,
389 such as XGBoost (eXtreme Gradient Boosting) (Chen & Guestrin, 2016). This is again a classification
390 algorithm that uses sequential iterations, where decision trees are combined to increase classification
391 accuracy.

392 Often QSPRs exploit similarity-based classification, since compounds with similar molecular
393 structures are expected to have similar properties. These methods calculate distance measures to
394 provide a classification in terms of similarity among samples. The most known approach in this
395 framework is the k -Nearest Neighbors (k NN) classifier: it classifies a sample according to the most
396 frequent class of its k most similar training samples (Kowalski & Bender, 1972). The N3 (N -Nearest

397 Neighbors) approach is an evolution of k NN, which uses locally-weighted information to classify
398 new samples. The Binned Nearest Neighbors (BNN) method is similar to k NN, but the prediction is
399 based on a flexible number of neighbors (Todeschini *et al.*, 2015a).

400 Another classification approach, which is relatively frequent in QSPR applications, is the Support
401 Vector Machine (SVM) method (Vapnik, 1998). It defines the boundary between two classes by
402 maximizing the distance between the support vectors and the decision boundary, where support
403 vectors are those training samples located in the proximity of the class border. Moreover, SVM can
404 use non-linear kernel functions for defining non-linear decision boundaries.

405 To visually exemplify the different ways classification methods can define boundaries between
406 classes, a dataset of 324 chemicals was generated from the ChemTastesDB database (Rojas *et al.*,
407 2022), including 61 chemicals labelled as sweeteners and 263 as bitterants. Their molecular structures
408 were encoded through the binary molecular access system (MACCS) keys (Durant *et al.*, 2002). The
409 chemical space was represented by the first two t-Distributed Stochastic Neighbor Embedding (t-
410 SNE) dimensions (van der Maaten & Hinton, 2008), calculated by using the Jaccard-Tanimoto metric
411 as the distance measure (Todeschini *et al.*, 2015b). Finally, different classification approaches were
412 calculated to show how the class boundaries can vary in a 2D space according to the adopted method
413 (Figure 2). SIMCA and PFs, which are class-modeling approaches, define a boundary around the
414 target class (sweet class in this example), while the discriminant methods, for instance, LDA, QDA
415 and PLSDA, divide the entire chemical space into two sub-spaces, each associated with one of the
416 two modeled classes, with linear or non-linear boundaries, depending on the adopted classification
417 algorithm.

418
419 **Figure 2 should be inserted around here**

420

421 1.2.2. Classification measures

422 QSPR models must be assessed through measures of goodness-of-fit and goodness-of-prediction. In
423 this framework, several indices can be used to evaluate the quality of models, which are based on the
424 number of misclassifications (molecules assigned to the wrong class) (Ballabio *et al.*, 2018).
425 Classification metrics are derived from the confusion matrix, which is a square matrix with
426 dimensions $G \times G$, where G is the number of modeled classes. Each entry c_{gk} of this matrix represents
427 the number of samples belonging to class g and assigned to class k . Consequently, the diagonal
428 elements c_{gg} denote the counts of the correctly classified samples while the off-diagonal elements
429 represent those erroneously classified. In the simplest binary case where two classes (positive and

430 negative) are modeled, the confusion matrix is a 2×2 numerical table with four entries labelled as
 431 follows: true positive and true negative (TP and TN, the number of positive and negative samples
 432 correctly classified, respectively), false positive (FP, the number of negative samples classified as
 433 positive) and false negative (FN, the number of positive samples classified as negative).

434 The most common classification measures derived from the confusion matrix are *sensitivity* (Sn_g),
 435 *precision* (Pr_g), *specificity* (Sp_g), as well as their combination, such as the *F-score* (F_g) (also known
 436 as the *F1-score* or *F-measure*). These indices are associated to each modeled g -th class and defined
 437 as:

$$\begin{aligned}
 Sn_g &= \frac{c_{gg}}{n_g} & Pr_g &= \frac{c_{gg}}{n'_g} \\
 Sp_g &= \frac{\sum_{\substack{k=1 \\ k \neq g}}^G (n_k - c_{kg})}{n - n_g} & F_g &= 2 \cdot \frac{Sn_g \cdot Pr_g}{Sn_g + Pr_g}
 \end{aligned} \tag{2}$$

439 where n_g is the number of samples of the g -th class, n'_g is the number of samples that are classified
 440 in the g -th class and n is the total number of samples. Higher values of sensitivity, specificity and
 441 precision are associated with better class discrimination.

442 Beside measures assigned to each class, global classification indices have been proposed to provide
 443 an overall assessment of the discrimination ability of classifiers. The *Non-Error Rate* (*NER*, also
 444 called *balanced accuracy* or *recall*) corresponds to the arithmetic mean of class sensitivities:

$$NER = \frac{\sum_{g=1}^G Sn_g}{G} \tag{3}$$

447 while *accuracy* corresponds to the fraction of correctly classified samples:

$$ACC = \frac{\sum_{g=1}^G c_{gg}}{n} \tag{4}$$

450 Note that accuracy is considered a biased estimate when classes are unbalanced, that is, samples are
 451 distributed in classes with significantly different frequencies.

452 Alternatively, classification performance can also be evaluated through the Matthew Correlation
 453 Coefficient (*MCC*), which ranges between -1 and 1 and has originally been defined to assess binary
 454 classification tasks:
 455

456
$$MCC = \frac{TP \cdot TN - FP \cdot FN}{\sqrt{(TP + FN) \cdot (TP + FP) \cdot (TN + FP) \cdot (TN + FN)}} \quad (5)$$

457

458 Another way to assess discrimination capability of classification models is through ROC (Receiver
459 Operating Characteristics) curves. These are graphic plots of *sensitivity* and *1 - specificity* (also known
460 as False Positive Rate, FPR) for a classification system when its discrimination threshold is changed.
461 For each threshold value, the corresponding TPR and FPR values are calculated. The optimal
462 classifier will provide a full ROC curve, while a random classification rule would give a line along
463 the diagonal of the ROC space. To quantitatively compare classification models through ROC curves,
464 a common approach is to calculate the area under the curve (*AUC*), also known as *AUROC* or *ROC-*
465 *AUC*.

466 **2. Classification models for taste prediction**

467 In this section, ligand-based (LB) classifiers for taste prediction are described. The classifiers were
468 retrieved from 52 published studies, which were found through critical screening of the Web of
469 Science citation indexing service. To the best of our knowledge, the first work published on this topic
470 was by Lemont B. Kier in 1980. In addition to the models described below, there are several
471 multicriteria reviews that are focused on QSAR-based prediction of tastes by means of diverse
472 classification-based machine learning approaches (De León *et al.*, 2021; Malavolta *et al.*, 2022; Rojas
473 *et al.*, 2016a; Spillane *et al.*, 1996; Walters, 2006). Ligand-based models are presented on the basis
474 of the basic tastes to be predicted.

475 **2.1. Sweet and bitter tastants**

476 The discrimination between sweet and bitter compounds has probably been the most important task
477 in quantitative structure-taste relationship studies. Twelve ligand-based (LB) models for the
478 discrimination of these two tastes are summarized in Table 1.

479

480 **Table 1 should be inserted around here**

481

482 Earlier studies had been focused on the use of simple modeling approaches, such as discriminant
483 analysis. In 1980, Kier (Kier, 1980) performed a two-variable linear discriminant analysis (LDA) to
484 discriminate sweet and bitter aldoximes taken from the data published by Acton and Stone (Acton &
485 Stone, 1976). For each class, 10 tastants were selected on the basis of the largest percentage of the
486 taste and the most potent taste response. Each molecule was represented by two connectivity indices

487 named $^1\chi$ and $^4\chi_p$. The classifier was used to predict the taste of nine external molecules, achieving
488 seven correct predictions, one incorrect prediction and one tastant labelled as ambiguous. After this
489 pioneering work, Takahashi and Miyashita's group (Miyashita *et al.*, 1986a; Takahashi *et al.*, 1984;
490 Takahashi *et al.*, 1982) developed new models, based on LDA and SIMCA. In the first study
491 (Takahashi *et al.*, 1982), three molecular descriptors were used to correctly classify 22 perillartines
492 (11 in each class) through a LDA classifier. In a subsequent study (Takahashi *et al.*, 1984), a test set
493 of nine compounds (five sweet and four bitter) retrieved from Acton's dataset (Acton & Stone, 1976)
494 was included. Two LDA classifiers, one based on three descriptors and one with just two descriptors,
495 were developed, achieving similar performances on both training and test sets. In the last study,
496 Miyashita (Miyashita *et al.*, 1986a) used 70 sweet and 21 bitter aspartyl dipeptides (L-Asp-NH-R)
497 to calibrate a five-variable SIMCA model.

498 Drew (Drew *et al.*, 1998) used a dataset of 21 sweeteners, 20 sweet/bitter and 9 bitter mono- and di-
499 substituted sodium sulfamates, which were properly optimized by the semiempirical PM3 method to
500 calculate 11 molecular descriptors. Then, they performed a discriminant analysis (DA), which was
501 able to perfectly discriminate all the compounds. In addition, a cluster analysis was carried out in the
502 space of the first two principal components, where a linear separation could be found only between
503 sweet and sweet/bitter tastants. Two years later, Spillane (Spillane *et al.*, 2002) synthesized and
504 characterized 23 meta-phenylsulfamate derivatives. The equilibrium geometry of the tastants were
505 obtained by means of the AM1 semi-empirical method, in such a way as to calculate diverse
506 descriptors, which were used to calibrate a discriminant plot, an LDA and a quadratic discriminant
507 analysis (QDA). The first model was obtained by plotting the values of length (x , Å) against the
508 volume V_{CPK} (xyz , Å³). The best LDA classifier was obtained with the x , width (z , Å), aqueous
509 solvation energy (E_{solv}) and HOMO descriptors; while the best QDA model used the x , z , E_{solv} and
510 LUMO descriptors. Among these models, the QDA exhibited the best performance in terms of the
511 *NER*. In a further analysis, these three models were used for predicting the taste of 9 unsynthesized
512 meta-compounds.

513 Other models to discriminate sweetness and bitterness were based on the k -Nearest Neighbors (k NN)
514 approach. The first model was proposed by Takahashi (Takahashi *et al.*, 1982) to classify 22
515 perillartines. The k NN method misclassified only two bitter molecules in the entire dataset. Several
516 years later, k NN was used by Rojas (Rojas *et al.*, 2016c) with 508 curated and filtered tastants (427
517 sweet and 81 bitter), which were split into training (356 tastants) and test sets (152 molecules).
518 Molecules were represented by means of 3,763 conformation-independent Dragon molecular
519 descriptors (Kode srl., 2018), which were initially analyzed by means of the V-WSP unsupervised

520 variable reduction approach (Ballabio *et al.*, 2014). Then, the training set was used for model
521 development using the 5-fold cross-validation approach to determine the optimal k value during the
522 genetic algorithms-variable subset selection (GAs-VSS). A four-descriptor model was selected as
523 optimal, with a balanced performance in prediction ($NER = 0.789$, $Sn_{sweet} = 0.953$ and $Sn_{bitter} = 0.625$).
524 In addition, the applicability domain (AD) of the model was calculated. In a further analysis, the
525 sweeteners database was used to perform a quantitative structure-property relationship (QSPR) for
526 predicting the relative sweetness (RS) or sweetness potency (Sw) of the sweeteners (Rojas *et al.*,
527 2016b).

528 Starting from 2017, the random forest (RF) classifier started to be applied to discriminate sweet and
529 bitter tastants. Chéron (Chéron *et al.*, 2017) merged 316 sweeteners from SweetenersDB and 680
530 bitterants from the BitterDB (Wiener *et al.*, 2012), which were represented by 244 conformation-
531 independent Dragon descriptors (Kode srl., 2018). One hundred trees with a tree depth of five
532 molecular descriptors and the Gini splitting criterion were set up during the calibration of the RF
533 classifier, which exhibited good performance on the test set, constituted by the 20% of tastants (NER
534 $= 0.914$ and $MCC = 0.848$). In a further analysis, the model was used to identify 4,585 natural
535 molecules of the SuperNatural II database (Banerjee *et al.*, 2015) as potential sweet agents and their
536 relative sweetness was predicted by means of a support vector regression (SVR). One year later,
537 Banerjee and Preissner (Banerjee & Preissner, 2018) calibrated a RF model, named
538 BitterSweetForest, for 517 sweeteners from SuperSweet (Ahmed *et al.*, 2011) and 685 bitterants from
539 the BitterDB (Wiener *et al.*, 2012). Compounds were represented by means of the extended
540 connectivity fingerprints ECFP4 (Morgan, 1965; Rogers & Hahn, 2010) calculated using RDKit. The
541 best model achieved good predictive ability of the 241 test set molecules ($AUC = 0.98$, $F\text{-score} =$
542 0.92 , $ACC = 0.967$, and $Cohen's\ Kappa = 0.92$). In addition, the BitterSweetForest model was used
543 to virtually screen the SuperNatural II (Banerjee *et al.*, 2015) and DrugBank databases. Goel (Goel
544 *et al.*, 2021) developed a dataset of 1,179 sweeteners and 743 bitterants (retrieved from the
545 BitterSweet database (Tuwani *et al.*, 2019)) and used the recursive feature elimination approach to
546 identify eight descriptors from 1,613 conformation-independent Mordred descriptors (Moriwaki *et*
547 *al.*, 2018). The best RF classifier exhibited good prediction on the test set (20% molecules), with NER
548 $= 0.855$, $ACC = 0.865$ and $MCC = 0.785$. In addition, 478 structurally diverse sweeteners (334 in the
549 training set and 144 in the test set) were used to predict the relative sweetness (log RS) by means of
550 a 3D regression-based RF model, which was then submitted to a molecular docking simulation to
551 calculate the binding conformation and associated free binding energy with the T1R2/T1R3 receptor.
552 In a subsequent step, compounds from the Universal Natural Products Database (UNPD) (Gu *et al.*,

553 2013) were virtually screened following the above mentioned workflow, which was coupled with
554 toxicity scaffold analysis as well.

555 Recently, other advanced classifiers were used for sweetness and bitterness discrimination. In 2022,
556 Bo (Bo *et al.*, 2022) curated a dataset of 797 bitterants and 1,249 sweeteners retrieved from the
557 BitterDB (Dagan-Wiener *et al.*, 2019), SuperSweet (Ahmed *et al.*, 2011) and FlavorDB. The 2D
558 RDKit molecular descriptors and fingerprints were used to calibrate multilayer perceptron (MLP)
559 models, while 2D-RGB color images (32×32 pixels) were used to train convolutional neural
560 networks (CNN). Among the three models, the best one (BitterSweetMLP-Fingerprint) was obtained
561 with 17 fingerprints (selected by means of the PCA using oblique rotation), with good performance
562 for predicting the 409 test set tastants ($NER = 0.880$, $AUC = 0.950$, $ACC = 0.880$, and $MCC = 0.750$).
563 Molecular charges and their surface interaction descriptors were retained since they were relevant for
564 classifying sweeteners/bitterants. Maroni (Maroni *et al.*, 2022) calibrated a gradient boosting machine
565 model (LightGBM implementation), along with other well-known classifiers: k NN, RF, logistic
566 regression (LR) and multilayer perceptron (MLP). These authors filtered and curated a database of
567 2,195 tastants, which were represented by 1,402 conformation-independent features calculated in the
568 RDkit, Pybel (O'Boyle *et al.*, 2008) and Mordred (Moriwaki *et al.*, 2018). A sequential descriptor
569 selection combined with hierarchical clustering in the descriptor's Spearman rank-order index was
570 used. The GBM classifier was optimal with good results in calibration ($NER = 0.893$, $AUC = 0.950$
571 and $F\text{-score} = 0.883$). Furthermore, the SHapley Additive exPlanations (SHAP) allowed the
572 identification of the most suitable descriptors.

573 2.2. Sweet and non-sweet tastants

574 Several classification-based machine learning models have been built to discriminate between sweet
575 and the non-sweet molecules, as well as to use them in order to predict and synthesize novel
576 sweeteners. Nineteen ligand-based classifiers for sweet taste predictions are summarized in Table 2.

577
578 **Table 2 should be inserted around here**

579
580 As presented in the sweet/bitter section, the sulfamate sweetness prediction was based on models
581 using biplot discriminant analysis (DA) published mainly by Spillane's research group. In the first
582 application, Spillane and McGlinchey (Spillane & McGlinchey, 1981) used the length (x , Å) and
583 volume V_{CPK} (xyz , Å³) descriptors to construct a DA-biplot for the discrimination of 47 sweet and
584 non-sweet carbosulfamate ($RNHSO_3^-$) derivatives. In a second study, Spillane and Sheahan (Spillane
585 & Sheahan, 1989) again used the x and V_{CPK} descriptors to classify 17 carbosulfamates. In a

586 subsequent DA-plot application (Spillane *et al.*, 1993), the V_{CPK} and $\Sigma\sigma$ descriptors were used for
587 40 synthesized ring disubstituted phenylsulfamates as sodium salts (no classification performances
588 were reported for this discriminant plot). Between 1983 and 2009, the same research group developed
589 six models based on linear discriminant analysis (LDA) and four models based on quadratic
590 discriminant analysis (QDA). In the first LDA application, 33 sweet and non-sweet heterosulfamates
591 were used (Spillane *et al.*, 1983). Twenty molecules were retrieved from the Acton's database (Acton
592 & Stone, 1976), while another 13 tastants were synthesized and evaluated by the authors for taste
593 sensation. The best model was composed of the length (x , Å), width (z , Å) and the first-order valence
594 connectivity index ($^1\chi^v$) descriptors. In a subsequent study, Spillane and Sheahan (Spillane &
595 Sheahan, 1989) used the same pool of descriptors to calibrate a LDA model for other 23
596 heterosulfamates and an extended dataset of 56 heterosulfamates.

597 Starting from 2000, the classification and regression tree (CART) method was also used for sweetness
598 prediction. Spillane (Spillane *et al.*, 2000) augmented previous datasets in order to include 101
599 heterosulfamate sodium salts (32 were synthesized for this study). The datasets contained 20
600 sweeteners and 81 non-sweet derivatives. LDA and QDA models were calibrated with four molecular
601 descriptors (x , y , z and $^1\chi^v$), while with CART, three features were used (x , y and $^1\chi^v$). Among
602 these models, the QDA classifier showed the best performance. Three years later, the dataset was
603 further augmented by including newly synthesized compounds (15 sweet and 16 non-sweet) (Spillane
604 *et al.*, 2003). In this case, CART provided better results than LDA and QDA using the y , z , V_{CPK} and
605 LUMO descriptors. In 2005, Kelly (Kelly *et al.*, 2005) merged 63 sweeteners available in the
606 literature with 19 cyclamate derivatives that were synthesized and tasted in this work. The sweetness
607 value was used to define three classes of the predominant tastes: non-sweet (0 to 39), sweet/non-
608 sweet (40 to 60) and sweet (61 to 100). The dataset was randomly split (maintaining the class
609 proportion) into a training set and a test set of 75 molecules and 8 molecules, respectively. In this
610 work, an external validation was used for the first time for the sweet/non-sweet discrimination. The
611 LDA and QDA models exhibited poor predictive ability, while CART based on six descriptors (x ,
612 HOMO, LUMO, E_{solv} , $V_{Spartan}$ and σ) exhibited acceptable prediction performance.

613 One year later, Spillane (Spillane *et al.*, 2006) developed three CART models to study a dataset of 82
614 tastants (42 newly synthesized disubstituted phenylsulfamates). The best classifier used 70 molecules
615 in the training set and 12 test set compounds randomly selected. Molecules in the test set were only
616 the newly synthesized non-sweet (11 compounds) and sweet/non-sweet (1 compound), while the four
617 newly synthesized sweeteners were placed in the training set. This model used seven descriptors and
618 provided good prediction ability. Finally, 28 five-membered aromatic ring thiazolyl-, benzothiazolyl-,

619 and thiadiazolylsulfamates were synthesized and merged together with 30 well-known heterocyclic
620 sulfamates to create a database (Spillane *et al.*, 2009). Compounds were grouped into three classes
621 according to the predominant taste: sweet, non-sweet and sweet/non-sweet. LDA and QDA were
622 initially used considering all the molecules as training chemicals. Then, the authors calibrated two
623 CART models by randomly splitting the dataset into a training set (48 tastants) and a test set (10
624 molecules). Between these two models, the best CART classifier used six descriptors and exhibited
625 a moderate performance when applied to the test set.

626 In another two studies, Miyashita's group (Miyashita *et al.*, 1986b; Okuyama *et al.*, 1988) also used
627 sulfamate derivatives to calibrate structure-taste relationships based on the SIMCA classifier. In the
628 first work, 14 sweet and 36 non-sweet carbosulfamates described by molar refractivity (MR), five
629 geometrical STERIMOL features and the Taft's σ^* descriptor were used (Miyashita *et al.*, 1986b).
630 The SIMCA model correctly predicted 13 sweet and 24 non-sweet molecules. In addition, a set of
631 alkyl groups were proposed as potential substituents, from which six alkylsulfamates were predicted
632 as potential sweeteners. Among these compounds, one was synthesized and exhibited a relative
633 sweetness of three times greater with respect to sucrose. Two years later, the same authors used 25
634 acyclic and 20 cyclic carbosulfamates represented by different graph theoretical invariants (Okuyama
635 *et al.*, 1988). In addition, the acyclic sulfamates were also represented by the weighted path numbers
636 for the rooted atom (path length from 1 to 8) and counts of self-returning walks for the rooted atom
637 (number of steps from 2 to 13), while the atomic path numbers for the rooted atom (path length from
638 1 to 8) and the counts of self-returning walks for the rooted atom were also computed for cyclic
639 sulfamates. In both cases, the SIMCA model achieved similar performance for the acyclic
640 carbosulfamates and the cyclic derivatives.

641 The first *k*NN model for the discrimination between sweet and non-sweet tastants was published in
642 2016 (Rojas *et al.*, 2016c). A nine-descriptor *k*NN model provided the best discrimination between
643 433 sweet and 133 tasteless curated molecules, with similar performances for training ($NER = 0.838$)
644 and test sets (30% of compounds), $NER = 0.752$. One year later, the same research group (Rojas *et al.*,
645 2017) developed an expert system that integrated unsupervised and supervised machine learning
646 approaches. To this end, a database of 435 sweet and 214 non-sweet (bitter and tasteless) molecules
647 were represented by means of 875 conformation-independent descriptors (Todeschini & Consonni,
648 2009) and extended connectivity fingerprints (ECFPs) (Rogers & Hahn, 2010), calculated by the
649 Dragon software (Kode srl., 2018). Similarity analysis was based on the ECFPs and multidimensional
650 scaling (MDS), while the supervised classification was carried out with the consensus predictions
651 provided by *N*-Nearest Neighbors (N3) and partial least squares discriminant analysis (PLSDA), with
652 good predictive accuracy on the test chemicals ($NER = 0.848$, non-assigned = 19.3%). A new

653 consensus model was published in 2019 by Zheng (Zheng *et al.*, 2019) for a curated database of 530
654 sweet and 850 non-sweet molecules, which were represented by four types of ECFPs (Rogers &
655 Hahn, 2010): 1024bit-ECFP4, 2048bit-ECFP4, 1024bit-ECFP6 and 2048bit-ECFP6. They used the
656 *k*NN classifier, along with support vector machine (SVM), random forest (RF), gradient boosting
657 machine (GBM) and deep neuron network (DNN) approaches to developed 1,312 individual models,
658 as well as 96 averaged classification models. As a result, four consensus models were constructed
659 (CM01 - CM04), and the best one (using 19 best individual models) was selected to construct the e-
660 Sweet model. This model achieved good results in predicting the 221 test set compounds (*NER* =
661 0.900, *F-score* = 0.878 and *MCC* = 0.807). In a further step, a consensus regression was developed
662 to predict the relative sweetness of 352 sweeteners.

663 In addition, Tuwani (Tuwani *et al.*, 2019) calibrated diverse models based on RF, ridge logistic
664 regression and AdaBoost for the classification of sweet/non-sweet and bitter/non-bitter molecules
665 (refer to bitter and non-bitter section). These models were named BitterSweet. For sweetness
666 prediction, a dataset of 1,205 sweeteners and 1,171 non-sweeteners were represented by means of
667 diverse molecular descriptors calculated in Dragon (Kode srl., 2018), Canvas (Schrödinger LLC,
668 2017) and ChemoPy (Cao *et al.*, 2013). The best model in terms of classification accuracy for the test
669 set (7% of molecules) used the 2D/3D Dragon descriptors reduced by means of the Boruta algorithm
670 and subsequently coupled with AB machine learning: *NER* = 0.834, *AUC* = 0.883 and *F-score* =
671 0.856.

672 Two years later, Fritz (Fritz *et al.*, 2021) developed the VirtualTaste prediction platform for predicting
673 the sweet taste of molecules based on the RF classifier (VirtualSweet model). The database included
674 2,011 sweet and non-sweet (bitter and tasteless) molecules that were curated and standardized from
675 the SuperSweet database (Ahmed *et al.*, 2011) and from their previous BitterSweetForest database
676 (Banerjee & Preissner, 2018). Molecules were represented by MACCS keys (Durant *et al.*, 2002) and
677 Morgan molecular fingerprints (Morgan, 1965; Rogers & Hahn, 2010). The RF model achieved good
678 external prediction on the 403 test set tastants (*NER* = 0.893, *AUC* = 0.951, *F-score* = 0.888 and *ACC*
679 = 0.893). Furthermore, the VirtualSweet model was used to virtually screen molecules from the
680 DrugBank database and from the SuperNatural II database (Banerjee *et al.*, 2015). One year later,
681 Yang (Yang *et al.*, 2022) used the RF and the XGBoost classifiers, along with other approaches, to
682 calibrate diverse models for a database named Taste DB. However, this name was previously
683 proposed by Ruddigkeit and Reymond (Ruddigkeit & Reymond, 2014). This dataset contained six
684 families of compounds: natural (973 sweeteners and 687 non-sweeteners), artificial (402 positive and
685 798 negative), carbohydrate (220 sweet and 238 non-sweet), non-carbohydrate (1,155 positive and
686 1,476 negative), nutritive (226 sweet and 268 non-sweet) and non-nutritive (1,149 positive and 1,464

687 negative). For validation purposes, the datasets were divided into training and test set in a proportion
688 of 8:2. The best artificial sweeteners model (in terms of accuracy for the test set prediction) used the
689 RF classifier and MACCS structural keys ($NER = 0.920$ and $AUC = 0.971$), while for the carbohydrate
690 family of compounds, the XGBoost approach and Atom pairs descriptors ($NER = 0.926$ and $AUC =$
691 0.974) were used. The remaining four models were developed by means of the XGBoost classifier
692 and MOE2d descriptors with the following performances for the test set: 1) natural molecules (NER
693 $= 0.841$ and $AUC = 0.920$); 2) non-carbohydrate compounds ($NER = 0.867$ and $AUC = 0.947$); 3)
694 nutritive sweeteners ($NER = 0.876$ and $AUC = 0.956$); and 4) non-nutritive molecules ($NER = 0.889$
695 and $AUC = 0.961$). In further analysis, these authors developed regression models to predict sweetness
696 potency ($\log Sw$).

697 More recently, Bo (Bo *et al.*, 2022) developed diverse quantitative structure-taste relationships based
698 on MLP and CNN deep learning classifiers, following the same workflow as previously described in
699 the sweet/bitter section. In this case, the dataset contained 1,119 sweeteners and 1,101 non-sweeteners
700 (tasteless and bitter). The best two models, in terms of their predictive ability, are the SweetMLP-
701 Fingerprint ($NER = 0.900$, $AUC = 0.940$, $ACC = 0.880$ and $MCC = 0.800$) and SweetCNN ($NER =$
702 0.850 , $AUC = 0.900$, $ACC = 0.840$ and $MCC = 0.660$). These models were used to predict the taste
703 of 902 tastants of the bitter data set. Lee (Lee *et al.*, 2022) used a fully connected network (FCN),
704 along the RF, XGB and LGBM classifiers, to propose the soft-vote ensemble approach. The curated
705 dataset included 1,237 sweeteners and 1,054 non-sweeteners retrieved from the BitterSweet database
706 (Tuwani *et al.*, 2019), which were represented by means of eight 2D fingerprints and diverse
707 molecular descriptors. Among the 44 different models, the best models were LGBM applied to
708 layered fingerprints and alvaDesc descriptors (Mauri & Bertola, 2022). These two models were used
709 to assemble the BoostSweet model for sweetness prediction by means of the soft-vote method that
710 averages the prediction of each model. The BoostSweet classifiers achieved good performance for
711 the test set (211 sweeteners and 248 non-sweeteners): $NER = 0.899$, $AUC = 0.961$ and $F-score =$
712 0.907 .

713 **2.3. Bitter and non-bitter tastants**

714 The prediction of sweetness has been the predominant goal for research in the computational taste
715 framework, probably because bitterness was usually linked to toxic compounds (as described for the
716 alkaloids). However, in the last few years, models that predict bitterness have received considerably
717 more attention due to the use of bitterants in several applications, particularly in food and
718 pharmaceutical industries. In contrast to the sweet/bitter models, where the main purpose was
719 sweetness prediction, comprehensive classification models for bitterness prediction are focused on

720 discriminating bitter from non-bitter tastants. The 14 ligand-based models found to date in the
721 literature are summarized in Table 3.

722
723 **Table 3 should be inserted around here**

724
725 In 2006 Rodgers (Rodgers *et al.*, 2006) used the Naïve Bayes (NB) classifier for the bitterness
726 prediction of small molecules. The curated dataset was composed of 649 bitterant taken from
727 scientific literature and patents, and 13,530 hypothetical non-bitter molecules randomly selected from
728 the MDL Drug Data Repository (MDDR). All the compounds were represented by MOLPRINT 2D
729 circular fingerprints (aka Atom Environments) (Bender *et al.*, 2004), which were subjected to a
730 variable subset selection. Ten years later, Huang released the first online tool, namely BitterX (Huang
731 *et al.*, 2016), for bitterness prediction based on support vector machine (SVM) classifiers. Data of
732 bitterants and bitterant-TAS2R interactions were retrieved from the PubMed (Sayers *et al.*, 2021) and
733 BitterDB (Wiener *et al.*, 2012) databases. In this work, a ligand-based model and a receptor-based
734 model were developed. In both cases, datasets were randomly split into training (80%) and test sets
735 (20%) three times to avoid bias in the data splitting, while genetic algorithms (GAs) were used for
736 the supervised descriptor selection. The ligand-based model was developed from a database of 539
737 bitterant and 539 non-bitter molecules and 46 physicochemical descriptors. The mean accuracy and
738 the area under the curve used in the prediction of the three models were $ACC = 0.915$ and $AUC =$
739 0.950 . On the other hand, the TAS2R receptor recognition model used 260 bitterants and 260 non-
740 bitter molecules (negative), and 20 physicochemical and 15 receptor descriptors with slightly lower
741 prediction quality ($ACC = 0.798$ and $AUC = 0.823$).

742 RF classifiers were also used for bitterness prediction (Fritz *et al.*, 2021; Tuwani *et al.*, 2019). Tuwani
743 published the BitterSweet model (Tuwani *et al.*, 2019) for the classification of bitterants, in which
744 they followed the same workflow as presented in the sweet/non-sweet section. The RF classifier,
745 coupled with PCA reduction of ChemoPy descriptors, achieved a higher non-error rate in prediction
746 for the test set (154 molecules): $NER = 0.819$, $AUC = 0.880$ and $F-score = 0.838$. This was then used
747 to predict the taste of external molecules available in the FlavorDB, FooDB, SuperSweet (Ahmed *et*
748 *al.*, 2011), Super Natural II (Banerjee *et al.*, 2015), DSSTox (Richard & Williams, 2002) and
749 DrugBank libraries. In a further analysis, molecular taste of Bitter new, UNIMI set and Phytochemical
750 dictionary databases (Dagan-Wiener *et al.*, 2017) were also predicted. Fritz (Fritz *et al.*, 2021)
751 implemented the VirtualBitter model following the same workflow as for the sweetness prediction
752 (refer to the sweet and non-sweet section). They retrieved molecules from the BitterDB (Dagan-
753 Wiener *et al.*, 2019) and from their BitterSweetForest model (Banerjee & Preissner, 2018), in order

754 to model 1,612 bitterants and non-bitter (sweet and tasteless) molecules. The RF classifier exhibited
755 acceptable performances in prediction (20% test compounds): $NER = 0.898$, $AUC = 0.956$, $F\text{-score}$
756 $= 0.882$ and $ACC = 0.901$. In addition, when a molecule is predicted as bitterant, the webserver
757 provides the potential bitter target prediction for the 25 human bitter receptors (hTAS2Rs) based on
758 a similarity-based analysis. Finally, the VirtualBitter model was used to virtually screen diverse
759 molecules from the DrugBank database and the SuperNatural II database (Banerjee *et al.*, 2015).
760 Between 2020 and 2021, Charoenkwan's group published three webserver for taste prediction of a
761 curated database of 320 bitter peptides and 320 non-bitter peptides (BTP640), randomly generated
762 from BIOPEP (Minkiewicz *et al.*, 2008). The dataset was split into a training set and a test set (80:20).
763 NB and RF classifiers as well as several other classifiers were used: kNN , scoring card method
764 (SCM), bidirectional encoder representation from transformers (BERT), support vector machine
765 (SVM), decision tree (DT), extremely randomized trees (ETree), linear support vector classifier
766 (SVC), logistic regression (LR), multi-layer perceptron (MLP) and extreme gradient boosting (XGB).
767 The SCM classifier (Huang *et al.*, 2012), which was used through the dipeptide propensity score
768 (PDS) and optimized with GAs, achieved good results in prediction ($ACC = 0.844$, $AUC = 0.904$ and
769 $MCC = 0.688$) when compared to the SVM, RF, NB, kNN and DT, and it was included in the iBitter-
770 SCM webserver application (Charoenkwan *et al.*, 2020a). The authors stated that iBitter-SCM
771 constituted a useful tool for the high-throughput prediction and *de novo* design of novel bitterant
772 peptides. Another webserver, named BERT4Bitter (Charoenkwan *et al.*, 2021a), automatically
773 generates feature descriptors for peptides through the BERT algorithm. This model achieved the best
774 test set performance ($ACC = 0.922$, $AUC = 0.964$ and $MCC = 0.844$) with respect to the other
775 calibrated classifiers (DT, ETree, kNN , SVC, LR, MLP, NB, RF, SVM and XGB). For the webserver
776 iBitter-Fuse (Charoenkwan *et al.*, 2021b), five groups of molecular features were calculated: 20
777 amino acid composition (AAC), 400 dipeptide composition (DPC), 21 pseudo amino acid
778 composition (PAAC), 22 amphiphilic pseudo amino acid composition (APAAC), 531
779 physicochemical properties from AAindex (AAI), as well as a new group achieved by fusing features
780 (994 descriptors). Ten SVM models were calculated, providing excellent prediction quality ($ACC =$
781 0.930 , $AUC = 0.933$ and $MCC = 0.859$). As described in their previous work, the authors calibrated
782 other machine learning models and demonstrated that the iBitter-Fuse model was superior in any case
783 (refer to Table 3 for the comparison between the iBitter-Fuse and the iBitter-SCM and BERT4Bitter
784 classifiers).

785 Dagan-Wiener used the Adaptive Boosting (AdaBoost) classifier for the first time in this framework
786 to create the BitterPredict model (Dagan-Wiener *et al.*, 2017). The dataset was composed of 691
787 bitterants (632 from the BitterDB (Wiener *et al.*, 2012)) and 1,917 non-bitter compounds retrieved

788 from several sources, which included 1,360 non-bitter flavors, 336 sweeteners, 186 tasteless
789 molecules and 35 molecules labelled as non-bitter (molecules not described by the word bitter in the
790 source). Each compound was represented by 59 molecular descriptors. The model was finally trained
791 with 16 molecular descriptors and demonstrated predictive ability for the test set (30% of molecules)
792 with $NER = 0.812$ and $ACC = 0.832$. Subsequently, the bitter class was evaluated for three external
793 datasets, namely Bitter New ($Sn = 0.739$), UNIMI set ($Sn = 0.783$) and Phytochemical Dictionary
794 (Baxter *et al.*, 1999) ($Sn = 0.980$ and $Sp = 0.692$). In a further step, the BitterPredict classifier was
795 applied to achieve prospective predictions of compounds from the FooDB, DrugBank, ChEBI and
796 the database of natural products. One year later, Zheng (Zheng *et al.*, 2018) developed several models
797 based on the gradient boosting machine (GBM), as well as k NN, SVM, RF and two deep neuron
798 networks (DNN2 and DNN3). These authors used a curated dataset of 707 bitterants and 592 non-
799 bitter compounds (132 tasteless, 17 non-bitter and 443 sweet). Molecules were represented by means
800 of several extended connectivity fingerprints (ECFPs): 1024bit-ECFP4, 2048bit-ECFP4, 1024bit-
801 ECFP6 and 2048bit-ECFP6. In order to avoid bias due to partition, the splitting of the dataset was
802 repeated 19 times for the k NN, SVM, GBM and RF models, and three times for the DNN2 and DNN3
803 models. Thus, 1,312 individual models and 96 average models were calibrated and consensus voting
804 was used to obtain nine models (CM01 - CM09), which were integrated in the server e-Bitter tool.
805 The best model (CM01) exhibited the following parameters for the test set (20% of compounds): F -
806 $score = 0.936$, $ACC = 0.929$ and $MCC = 0.856$.

807 The XGBoost classifier was also used for bitterness prediction. Margulis proposed the BitterIntense
808 model (Margulis *et al.*, 2021) for the classification of bitter molecules into very bitter and non-very
809 bitter (including non-bitter) classes. A dataset of 721 compounds were obtained from behavioral
810 studies using the rat brief access taste aversion (BATA), BitterDB (Dagan-Wiener *et al.*, 2019),
811 Analyticon repository of natural compounds on Kaggle, as well as from their previous dataset
812 BitterPredict (Dagan-Wiener *et al.*, 2017). Subsequently, 3D structures were used to calculate Canvas
813 molecular descriptors (Schrödinger LLC, 2017) and QikProp features (ADME descriptors)
814 (Schrödinger LLC, 2015). The XGBoost model achieved acceptable prediction on the test set (105
815 tastants): $NER = 0.790$, F - $score = 0.700$ and $ACC = 0.800$. Moreover, the BitterIntense model was
816 used for analyzing the connection between toxicity and the level of bitterness of molecules, as well
817 as for potential repurposing of COVID-19 targets. Independently, Bai developed the Children's Bitter
818 Drug Prediction System' (CBDPS) (Bai *et al.*, 2021) for the bitterness prediction of medicines. The
819 experimental dataset was retrieved from published works and the BitterDB (Dagan-Wiener *et al.*,
820 2019), which consisted of 1,732 tastants with a balanced number between bitter and non-bitter tastants
821 (ratio of 1:1). Then, 166 MACCS structural keys and 114 ChemoPy descriptors (Cao *et al.*, 2013)

822 were used to calibrate four models based on the XGBoost and RF classifiers. Among these models,
823 the optimal one was obtained with the XGBoost classifier and the MACCS structural keys, and
824 achieved the following performance in cross-validation: $F\text{-score} = 0.881$ and $ACC = 0.882$. In a last
825 step, the CBDPS model was applied to the screening of the external dataset of 222 children's oral
826 medicines.

827 The XGBoost classifier was also applied to develop the BitterMatch model (Margulis *et al.*, 2022).
828 A curated dataset of 303 bitterants resulted in 4,501 pairs of ligand-receptor associations (740
829 positives and 3,761 negatives). Optimized bitterants were used to calculate Canvas descriptors
830 (Schrödinger LLC, 2017), while 3 sets of features were computed for receptors. The BitterMatch
831 algorithm was divided into two scenarios: *filling the gaps* and *new ligands*. In both cases, 20% of the
832 molecules were considered as test sets, keeping in mind the proportion of the classes (repeated 100
833 times). In *filling the gaps*, the best model included chemical properties and neighbor-informed
834 chemical similarity features with an average recall-precision of 0.759. In contrast, the *new ligands*
835 scenario considered only chemical properties of ligands and receptors, as well as neighbors-informed
836 ligand similarity features (average recall-precision of 0.699). Afterwards, it was used to predict
837 associations for 12 external bitterants and drugs from the DrugBank.

838 More recently, Bo (Bo *et al.*, 2022) calibrated quantitative structure-taste relationships based on MLP
839 and CNN deep learning classifiers (as described before in the sweet/bitter and sweet/non-sweet
840 sections). In this work, a dataset of 797 bitterants and 1,436 non-bitterants (sweet and tasteless) was
841 used. The BitterMLP-Descriptor classifier with seven RDKit descriptors exhibited similar validation
842 performance ($NER = 0.820$, $AUC = 0.940$, $ACC = 0.840$ and $MCC = 0.660$) with respect to the
843 BitterCNN classifier ($NER = 0.790$, $AUC = 0.880$, $ACC = 0.810$ and $MCC = 0.600$). As described in
844 the sweet/non-sweet models, these two classifiers were used to analyze 1,229 tastants from the sweet
845 data set. De León (De León *et al.*, 2022) calibrated SVM, RF, AdaBoost and k NN models for a curated
846 dataset of 932 bitterants and 1,908 non-bitter molecules retrieved from BitterDB (Dagan-Wiener *et*
847 *al.*, 2019), Fenaroli's Handbook of flavours (Burdock, 2010) and the dataset of Rojas (Rojas *et al.*,
848 2016c). The compounds were represented by ECFPs and 22 selected Mordred descriptors (Moriwaki
849 *et al.*, 2018) on the basis of their probability density. For validation purposes, 20% of the molecules
850 were included in the test set. The two best classifiers turned out to be SVM ($ACC_{train} = 0.836$ and
851 $ACC_{test} = 0.870$) and AdaBoost ($ACC_{train} = 0.842$ and $ACC_{test} = 0.847$) based on ECFPs and
852 descriptors, respectively. In addition, the UNIMI dataset (Dagan-Wiener *et al.*, 2017) was used as the
853 external set to validate the performance of Premexotac models.

854 **2.4. Umami and non-umami tastants**

855 There are fewer ligand-based (LB) machine learning models that have been developed for the
856 discrimination between umami and non-umami peptides. This could be due to the higher complexity
857 of sensory evaluation and related costs than those related to the evaluation of sweet and bitter
858 molecules.

859 For the first model, named iUmami-SCM (Charoenkwan *et al.*, 2020b), the experimental information
860 for umami peptides was retrieved from the literature and from the BIOPEP-UWM database, while
861 bitter peptides, previously studied by the authors, were considered as non-umami molecules. The
862 UMP442 database (140 umami and 302 non-umami peptides) was used to calibrate a SCM classifier
863 based on a dipeptide propensity score (PDS), as described in the iBitter-SCM model (Charoenkwan
864 *et al.*, 2020a). The best model achieved good results in prediction (20% of test molecules): $AUC =$
865 0.898 , $ACC = 0.865$, $MCC = 0.679$, $Sn = 0.714$ and $Sp = 0.934$. In addition, the model's performance
866 was compared with six ML classifiers (SVM, RF, MLP, NB, kNN and DT). In the second application,
867 the same group of Charoenkwan combined six well-known ML classifiers (ETree, kNN , LR, PLS,
868 RF and SVM) in the UMPred-FRL model (Charoenkwan *et al.*, 2021c). To this end, they used
869 molecules of the UMP442 database (Charoenkwan *et al.*, 2020b), which were represented by seven
870 feature descriptors: amino acid composition (AAC), amphiphilic pseudo-amino acid composition
871 (APAAC), dipeptide composition (DPC), composition (CTDC), transition (CTDT), distribution
872 (CTDD) and pseudo-amino acid composition (PAAC). The UMPred-FRL predictor was assembled
873 by the best 7 informative features (SVM-AAC, PLS-AAC, SVM-CTDC, RF-DPC, RF-CTDC, PLS-
874 APAAC and LRDPC), and exhibited better performances when compared to the iUmami-SCM
875 classifier prediction ($AUC = 0.919$, $ACC = 0.888$ and $MCC = 0.735$).

876 In 2022, Pallante developed the Virtuous Umami platform (Pallante *et al.*, 2022) for umami prediction
877 based on SVM classifiers and the Charoenkwan's UMP442 database (Charoenkwan *et al.*, 2020b).
878 Due to the unbalanced classes, umami peptides were randomly duplicated to balance the class
879 cardinalities. Subsequently, 1,613 conformation-independent Mordred features (Moriwaki *et al.*,
880 2018) were subjected to feature selection by means of different approaches, which were used to
881 calibrate diverse SVM models. The best prediction was achieved by consensus between two models
882 (12 features), which exhibited a slightly lower performance in prediction ($AUC = 0.850$, $F-score =$
883 0.793 and $ACC = 0.876$) when compared to the iUmami-SCM and UMPred-FRL predictors. The
884 effectiveness of the model was visually shown by means of t-SNE. Finally, the umami predictor was
885 used to virtually screen the FooDB, FlavorDB, PhenolExplorer, Natural Product Atlas and PhytoHub
886 databases.

887 Recently, Dutta proposed the identification of optimal sequential residue patterns for umami and
888 bitter peptides (Dutta *et al.*, 2022a). These authors used a curated database of 292 bitter and 146

889 umami compounds retrieved from Charoenkwan's UMP442 database (Charoenkwan *et al.*, 2020b)
890 and others sources. Each peptide was represented by the following coarse-grained representation:
891 hydrophobic (H), polar and hydrophilic (P), positively charged (+) and negatively charged (-).
892 Afterwards, seven libraries of peptides were created by repeating a fixed set of coarse-grained
893 patterns. To select the best length, the dataset of taste-labeled peptides was split into a training set
894 (80%) and a test set (20%) by means of stratified random sampling. A length of five ($N = 5$) was
895 selected as the best coarse-grained pattern, where bitter peptides were represented by one
896 hydrophobic followed by four polar residues (HPPPP), while umami peptides had two negative
897 followed by three polar residues (—PPP). In a further step, the authors tested this method by using
898 two bitter proteins (Patatin-T5 and Legumin-A), where 8 and 5 peptide sequences with the
899 aforementioned course-grain pattern were identified. This approach allowed the rapid screening and
900 identification of sequential information patterns hidden in long chain peptides and proteins, rather
901 than predicting the taste class of peptides (no classification performances were reported).

902 **2.5 Bitter, sweet and umami tastant**

903 Dutta developed the first deep learning classifier to discriminate among sweet, bitter and umami
904 tastants (Dutta *et al.*, 2022b). The curated dataset was composed of 1,938 bitterants, 2,079 sweeteners
905 and 98 umami compounds, which were retrieved from the ChemTastesDB database (Rojas *et al.*,
906 2022) and the BitterSweet dataset (Tuwani *et al.*, 2019). Afterwards, 102 RDKit molecular
907 descriptors were used after a filtering process. For pattern recognition, the authors developed two
908 chemical spaces based on PCA and t-SNE, along with a functional group analysis by computing the
909 frequency of predefined fragments. Then, a deep neural network (DNN) with two hidden layers of
910 100 neurons was trained with 200 epochs. For balancing the cardinality of the umami class, the
911 synthetic minority oversampling technique (SMOTE) for data augmentation was used. The DNN
912 model was interpreted by means of the Shapley additive explanations (SHAP). The DNN model
913 achieved good predictive performance (15% of compounds): $NER = 0.901$ and $ACC = 0.887$.
914 Moreover, a graph neural network (GNN) was also tested with a slightly lower quality on external
915 prediction ($NER = 0.865$ and $ACC = 0.896$). Independently, Xiu (Xiu *et al.*, 2022) used the
916 BitterSweet dataset (Tuwani *et al.*, 2019) to develop the PyUmami model, which combined sweet
917 and bitter classifiers based on multilayer perception (MLP) and Mordred descriptors. Then, the sweet-
918 MLP ($ACC = 0.830$ and $AUC = 0.897$) and bitter-MLP models ($ACC = 0.81$ and $AUC = 0.895$) were
919 used to predict the sweetness of 1,040 bitterants from the BitterDB, and the bitterness of 14,175
920 sweeteners from the SWEET-DB, respectively. Only 169 tastants predicted as both sweet/bitter by
921 the PyUmami model were submitted to docking analysis with the T1R2/T1R3 and hT2R1 receptors.

922 Finally, 18 targets were experimentally verified for sweet, bitter and umami intensities by means of
923 electronic tongue analysis, and only 8 tastants were predicted to be non-toxic by means of twelve
924 QSAR approaches and three virtual Adverse Outcome Pathway (vAOP) models.

925 **2.6. Sour and non-sour tastants**

926 Only one LB classifier for the discrimination between sour and non-sour compounds has been
927 proposed (Fritz *et al.*, 2021). Information of molecules was retrieved from ChEMBL (Gaulton *et al.*,
928 2012) and curated from the PubMed database (Sayers *et al.*, 2021). The dataset consisted of 1,347
929 compounds divided into a training set and a test set of 1,214 and 133 molecules, respectively. The
930 model, named VirtualSour, was a ligand-based approach considering the RF classifier integrated with
931 the augmented random data sampling method. The model achieved good results in cross-validation
932 ($NER = 0.955$, $AUC = 0.998$, $F\text{-score} = 0.980$ and $ACC = 0.978$), and prediction ($NER = 0.896$, AUC
933 $= 0.994$, $F\text{-score} = 0.842$ and $ACC = 0.977$).

934 **2.7 General trends in taste modelling**

935 When looking at the evolution of modelling approaches for predicting the different tastes, common
936 trends and tendencies can be seen. Figure 3 shows the number of molecules (included in both training
937 and test set) used for the development of structure-property models as a function of the publication
938 year, starting from the very beginning of the modelling era (1980) up to 2022. First of all, it is apparent
939 that the number of chemicals used to train or test QSAR models has greatly increased (note that the
940 y axis of Figure 3 is in \log_{10} units). While the first modeling attempts considered a few dozen
941 chemicals, the number increased to several hundreds from 2000 to 2010. In addition, models were
942 initially developed considering only small families of compounds (for instance aldoximes,
943 perillartines, aspartyl dipeptides and sulfamates), which established restricted chemical spaces for
944 only these types of compounds. The most relevant increase in the number of chemicals occurred after
945 2015, when scientists started to use several thousand molecules to develop new models for taste
946 prediction. Interestingly, the study for bitter prediction published by Rodgers in 2006 (Rodgers *et al.*,
947 2006) used 13,530 molecules randomly selected from the MDL Drug Data Repository under the
948 assumption that this was representative of the bitterness chemical space. However, these molecules
949 were not validated with experimental sensory data as considered in the most recently published works.

950
951 **Figure 3 should be inserted around here**

952

953 The large growth of the number of molecules used in the development of models that started in 2015
954 is probably due to several research groups who concentrated their efforts on creating more extensive
955 and comprehensive databases, such as SuperSweet (Ahmed *et al.*, 2011), BitterDB (Wiener *et al.*,
956 2012), ChEMBL (Gaulton *et al.*, 2012) and Super Natural II (Banerjee *et al.*, 2015). These databases
957 collected and cataloged a greater number of substances associated with their molecular structures and
958 experimental taste values, which enabled the subsequent development of models based on a
959 significantly higher number of chemicals in the years after 2015. These large databases included
960 heterogeneous molecules, which allowed the extension of chemical spaces and, in fact, some attempts
961 were made for virtual screening of potential new tastants in several available databases, which were
962 complemented, in some cases, with docking analysis and experimental sensory evaluation of the
963 elicited tastants.

964 Another general trend is related to the type of analyzed taste. Figure 3, shows that in the first 29 years
965 from the first model developed in 1980, sweetness was the principal interest. Within this modelling
966 framework, only models for the discrimination of sweet chemicals versus bitter or non-sweet
967 molecules were taken into account. Afterwards, due to the development of more comprehensive
968 databases, models for the prediction of bitterness were proposed in addition to sweetness. The interest
969 in bitterness prediction could be related to the increasing interest of using bitterants as food and
970 pharmaceutical additives along with other applications. Starting from 2020, umami prediction proved
971 to be another attractive topic in the scientific community. The increasing interest in modelling this
972 taste is mainly related to Asian research groups, due to the importance of umami in oriental
973 gastronomy. On the other hand, modelling of sourness and saltiness is limited by the reduced number
974 of molecules that imprint these tastes.

975 The increasing number of molecules used to model tastants also enabled a better estimation of
976 predictive performance; that is, the accuracy in the prediction of the taste of chemicals which were
977 not used for model training. Validation is fundamental in the development of QSARs and usually
978 consists of the use of some chemicals, with known experimental taste values but not involved in the
979 model training, as the test molecules. The first studies did not generally account for model validation.
980 Until 2016 less than 10 chemicals were used in a couple of studies to validate models for
981 discrimination between sweet and bitter tastants (Table 1), while for the classification of sweet and
982 non-sweet chemicals, no test compounds were considered until 2005 and just a few in the studies
983 published between 2006 and 2009 (Table 2). On the other hand, the number of substances used for
984 model validation has grown enormously in recent years and now, hundreds of molecules are normally
985 used for validation purposes.

986 Finally, the increasing availability of newly synthesized chemicals has influenced the type of machine
987 learning approaches that have been used to establish molecular structure-taste relationships. Initially
988 only simple classification algorithms were used (such as Discriminant Analysis and CART), whereas
989 in the last decade, advanced approaches have been frequently applied, such as RF, SVM, boosting
990 algorithms and Neural Networks. This is a general trend in the framework of machine learning, which
991 has been supported by the computational and technological advancements of the latest decades.
992 However, unlike traditional approaches, the newer and novel classification methods require a tuning
993 phase for the selection of optimal values of their hyperparameters. This tuning phase is executed by
994 optimizing the models on a further set of chemicals, usually named an evaluation set, which has to be
995 added to the training set (used for the learning phase) and the test set (used for the final validation
996 phase). Therefore, execution of the tuning phase requires a more extended number of chemicals for
997 their calculation.

998 It is interesting to note that although a very limited number of descriptors was used in the first
999 developed models, the evolution of modeling approaches has not caused a considerable increase in
1000 the complexity of the models. In many cases the total number of descriptors used for the development
1001 of models is measured in the 10s, and only a few hundred descriptors have been used in some models
1002 for the discrimination of sweet and non-sweet tastants. Of course, molecular fingerprints are a special
1003 case, since the thousands of binary bits they include have to be considered simultaneously as a holistic
1004 description of the molecular structure. As in other modelling frameworks, the limited number of
1005 descriptors is probably due to the maintenance of a correct balance between the model complexity,
1006 predictive ability and interpretability.

1007 In earlier models for sweet prediction, descriptors mainly related to molecular size and bulkiness were
1008 used while recently, quantum-chemical descriptors were considered as well as different types of
1009 fingerprints and descriptors calculated by means of different software including Dragon, RDKit,
1010 Mordred, Pybel, alvaDesc and MOE2d. From an analysis of the most frequent molecular descriptors
1011 in models for bitterness, the relevant structural features are the presence of carbon/oxygen groups,
1012 sugar moieties, quaternary carbon centers and highly branched carbon centers, physicochemical
1013 properties, specific properties of the molecular surface and hydrophobicity. More specifically, the
1014 bitterness of peptides is strongly related to composition of amino acids, dipeptides and pseudo amino
1015 acids. Finally, molecular descriptors used for modelling umami taste are mainly linked to the presence
1016 of hydrophilic amino acids with negative charge and low molecular weights. In addition, patterns in
1017 the scaffolds related to amino acid composition; specifically glutamic acid (Glu) and aspartic acid
1018 (Asp) amino acid, were found to be crucial for umami prediction of peptides.

1019 **3. Conclusions**

1020 In this paper, we present a logical, comprehensive and critical review of the current state of ligand-
1021 based models of quantitative structure-property relationships along with the history of the prediction
1022 of the taste of molecules. Models detailed here complement previously published reviews available
1023 in the literature. Although the main modeling applications presented in this review relate to the
1024 prediction of molecular sweetness and bitterness, there is a notable increase in the interest and
1025 proposed application of QSAR models for the prediction of umami and sour tastants. It is notable that
1026 many authors cited in this review attempted to use the largest possible databases of tastants, as well
1027 as to improve the chemical representation of these databases through the use of several molecular
1028 descriptors, structural keys and fingerprints. In addition, this review reflects the wide variety of
1029 machine learning approaches used by investigators in order to calibrate more general models used in
1030 the prediction of properties of new molecules. In the future, it is expected that *in silico* methods will
1031 increase the application of predictive models in food chemistry (foodinformatics) in order to better
1032 understand the mechanisms involved in taste prediction. In addition, predictive models may provide
1033 useful tools to discover new molecular tastants with potential uses as raw-materials or additives in
1034 the food and pharmaceutical industries. Finally, our recommendation to chemists involve in taste
1035 prediction is to develop the largest possible molecular tastant databases to be used with novel
1036 classifiers in order to develop models able to predict more than two classes at a time. This expanded
1037 capability will greatly advance the science of foodinformatics.

1038 **4. Declaration of Competing Interest**

1039 The authors declare that they have no known competing financial interests or personal relationships
1040 that could have appeared to influence the work reported in this paper.

1041 **5. Acknowledgements**

1042 This study was supported by the Vicerrectorado de Investigaciones from Universidad del Azuay. The
1043 authors thank Dr. Wayne R. Hanson for his valuable revision of the manuscript and for providing
1044 some useful comments for improving the technical quality.

1045 **6. References**

1046 Acton, E. M., & Stone, H. (1976). Potential new artificial sweetener from study of structure-taste
1047 relationships. *Science*, 193(4253), 584-586. <https://doi.org/10.1126/science.959816>

- 1048 Adler, E., Hoon, M. A., Mueller, K. L., Chandrashekar, J., Ryba, N. J., & Zuker, C. S. (2000). A
1049 novel family of mammalian taste receptors. *Cell*, *100*(6), 693-702.
1050 [https://doi.org/10.1016/S0092-8674\(00\)80705-9](https://doi.org/10.1016/S0092-8674(00)80705-9)
- 1051 Ahmed, J., Preissner, S., Dunkel, M., Worth, C. L., Eckert, A., & Preissner, R. (2011). SuperSweet-
1052 A resource on natural and artificial sweetening agents. *Nucleic Acids Research*, *39*, D377-
1053 D382. <https://doi.org/10.1093/nar/gkq917>
- 1054 Bai, G., Wu, T., Zhao, L., Wang, X., Li, S., & Ni, X. (2021). CBDPS 1.0: A Python GUI application
1055 for machine learning models to predict bitter-tasting children's oral medicines. *Chemical and*
1056 *Pharmaceutical Bulletin*, *69*, 989-994. <https://doi.org/10.1248/cpb.c20-00866>
- 1057 Baines, D., & Brown, M. (2016). Flavor enhancers: Characteristics and uses. In B. Caballero, P. M.
1058 Finglas & F. Toldrá (Eds.), *Encyclopedia of food and health*, vol. 2 (pp. 716-723). Oxford
1059 (UK): Academic Press.
- 1060 Ballabio, D., Consonni, V., Mauri, A., Claeys-Bruno, M., Sergent, M., & Todeschini, R. (2014). A
1061 novel variable reduction method adapted from space-filling designs. *Chemometrics and*
1062 *Intelligent Laboratory Systems*, *136*, 147-154.
1063 <https://doi.org/10.1016/j.chemolab.2014.05.010>
- 1064 Ballabio, D., Grisoni, F., & Todeschini, R. (2018). Multivariate comparison of classification
1065 performance measures. *Chemometrics and Intelligent Laboratory Systems*, *174*, 33-44.
1066 <https://doi.org/10.1016/j.chemolab.2017.12.004>
- 1067 Banerjee, P., Erehman, J., Gohlke, B.-O., Wilhelm, T., Preissner, R., & Dunkel, M. (2015). Super
1068 Natural II-A database of natural products. *Nucleic Acids Research*, *43*(D1), D935-D939.
1069 <https://doi.org/10.1093/nar/gku886>
- 1070 Banerjee, P., & Preissner, R. (2018). BitterSweetForest: A random forest based binary classifier to
1071 predict bitterness and sweetness of chemical compounds. *Frontiers in Chemistry*, *6*, 93.
1072 <https://doi.org/10.3389/fchem.2018.00093>
- 1073 Barker, M., & Rayens, W. (2003). Partial least squares for discrimination. *Journal of Chemometrics*,
1074 *17*, 166-173. <https://doi.org/10.1002/cem.785>
- 1075 Baxter, H., Harborne, J. B., & Moss, G. P. (1999). *Phytochemical dictionary: A handbook of bioactive*
1076 *compounds from plants* (Second ed.). Boca Raton, USA: CRC press.
- 1077 Bayer, S., Mayer, A. I., Borgonovo, G., Morini, G., Di Pizio, A., & Bassoli, A. (2021).
1078 Chemoinformatics view on bitter taste receptor agonists in food. *Journal of Agricultural and*
1079 *Food Chemistry*, *69*(46), 13916-13924. <https://doi.org/10.1021/acs.jafc.1c05057>
- 1080 Behrens, M., & Ziegler, F. (2020). Structure-function analyses of human bitter taste receptors-where
1081 do we stand? *Molecules*, *25*(19), 4423. <https://doi.org/10.3390/molecules25194423>

1082 Bender, A., Mussa, H. Y., Glen, R. C., & Reiling, S. (2004). Similarity searching of chemical
1083 databases using atom environment descriptors (MOLPRINT 2D): evaluation of performance.
1084 *Journal of Chemical Information and Computer Sciences*, 44(5), 1708-1718.
1085 <https://doi.org/10.1021/ci0498719>

1086 Bo, W., Qin, D., Zheng, X., Wang, Y., Ding, B., Li, Y., & Liang, G. (2022). Prediction of bitterant
1087 and sweetener using structure-taste relationship models based on an artificial neural network.
1088 *Food Research International*, 153, 110974. <https://doi.org/10.1016/j.foodres.2022.110974>

1089 Breiman, L. (2001). Random forests. *Machine learning*, 45, 5-32.

1090 Breiman, L. J., Friedman, J. H., Olsen, R., & Stone, C. (1984). *Classification and regression trees*.
1091 California (USA): Wadsworth, Belmont

1092 Brereton, R. G. (2011). One- class classifiers. *Journal of Chemometrics*, 25, 225-246.
1093 <https://doi.org/10.1002/cem.1397>

1094 Brereton, R. G., & Lloyd, G. R. (2014). Partial least squares discriminant analysis: Taking the magic
1095 away. *Journal of Chemometrics*, 28, 213-225. <https://doi.org/10.1002/cem.2609>

1096 Breslin, P., & Huang, L. (2006). Human Taste: Peripheral Anatomy, tastetransduction, and coding.
1097 In T. Hummel & A. Welge-Lüssen (Eds.), *Taste and smell*, (pp. 152-190): KARGER.

1098 Brockhoff, A., Behrens, M., Roudnitzky, N., Appendino, G., Avonto, C., & Meyerhof, W. (2011).
1099 Receptor agonism and antagonism of dietary bitter compounds. *Journal of Neuroscience*,
1100 31(41), 14775-14782. <https://doi.org/10.1523/JNEUROSCI.2923-11.2011>

1101 Burdock, G. A. (2010). *Fenaroli's handbook of flavor ingredients*. Boca Ratón, USA: CRC Press.

1102 Cao, D.-S., Xu, Q.-S., Hu, Q.-N., & Liang, Y.-Z. (2013). ChemoPy: Freely available python package
1103 for computational biology and chemoinformatics. *Bioinformatics*, 29(8), 1092-1094.
1104 <https://doi.org/10.1093/bioinformatics/btt105>

1105 Chandrashekar, J., Hoon, M. A., Ryba, N. J. P., & Zuker, C. S. (2006). The receptors and cells for
1106 mammalian taste. *Nature*, 444, 288-294. <https://doi.org/10.1038/nature05401>

1107 Charoenkwan, P., Yana, J., Schaduengrat, N., Nantasenamat, C., Hasan, M. M., & Shoombuatong,
1108 W. (2020a). iBitter-SCM: Identification and characterization of bitter peptides using a scoring
1109 card method with propensity scores of dipeptides. *Genomics*, 112(4), 2813-2822.
1110 <https://doi.org/10.1016/j.ygeno.2020.03.019>

1111 Charoenkwan, P., Yana, J., Nantasenamat, C., Hasan, M. M., & Shoombuatong, W. (2020b).
1112 iUmami-SCM: A novel sequence-based predictor for prediction and analysis of umami
1113 peptides using a scoring card method with propensity scores of dipeptides. *Journal of*
1114 *Chemical Information and Modeling*, 60(12), 6666-6678.
1115 <https://doi.org/10.1021/acs.jcim.0c00707>

- 1116 Charoenkwan, P., Nantasenamat, C., Hasan, M. M., Manavalan, B., & Shoombuatong, W. (2021a).
1117 BERT4Bitter: A bidirectional encoder representations from transformers (BERT)-based
1118 model for improving the prediction of bitter peptides. *Bioinformatics*, 37(17), 2556-2562.
1119 <https://doi.org/10.1093/bioinformatics/btab133>
- 1120 Charoenkwan, P., Nantasenamat, C., Hasan, M., Moni, M. A., Lio, P., & Shoombuatong, W. (2021b).
1121 iBitter-fuse: A novel sequence-based bitter peptide predictor by fusing multi-view features.
1122 *International Journal of Molecular Sciences*, 22(16), 8958.
1123 <https://doi.org/10.3390/ijms22168958>
- 1124 Charoenkwan, P., Nantasenamat, C., Hasan, M. M., Moni, M. A., Manavalan, B., & Shoombuatong,
1125 W. (2021c). UMPred-FRL: A new approach for accurate prediction of umami peptides using
1126 feature representation learning. *International Journal of Molecular Sciences*, 22, 13124.
1127 <https://doi.org/10.3390/ijms222313124>
- 1128 Chattopadhyay, S., Raychaudhuri, U., & Chakraborty, R. (2014). Artificial sweeteners—A review.
1129 *Journal of Food Science and Technology*, 51, 611-621. [https://doi.org/10.1007/s13197-011-](https://doi.org/10.1007/s13197-011-0571-1)
1130 [0571-1](https://doi.org/10.1007/s13197-011-0571-1)
- 1131 Chaudhari, N., Pereira, E., & Roper, S. D. (2009). Taste receptors for umami: The case for multiple
1132 receptors. *The American Journal of Clinical Nutrition*, 90(3), 738S-742S.
1133 <https://doi.org/10.3945/ajcn.2009.27462H>
- 1134 Chen, T., & Guestrin, C. (2016). Xgboost: A scalable tree boosting system. *KDD '16: Proceedings*
1135 *of the 22nd ACM SIGKDD International Conference on Knowledge Discovery and Data*, 785-
1136 794. <https://doi.org/10.1145/2939672.2939785>
- 1137 Chéron, J.-B., Casciuc, I., Golebiowski, J., Antonczak, S., & Fiorucci, S. (2017). Sweetness
1138 prediction of natural compounds. *Food Chemistry*, 221, 1421-1425.
1139 <https://doi.org/10.1016/j.foodchem.2016.10.145>
- 1140 Dagan-Wiener, A., Nissim, I., Abu, N. B., Borgonovo, G., Bassoli, A., & Niv, M. Y. (2017). Bitter
1141 or not? BitterPredict, a tool for predicting taste from chemical structure. *Scientific Reports*, 7,
1142 12074. <https://doi.org/10.1038/s41598-017-12359-7>
- 1143 Dagan-Wiener, A., Di Pizio, A., Nissim, I., Bahia, M. S., Dubovski, N., Margulis, E., & Niv, M. Y.
1144 (2019). BitterDB: Taste ligands and receptors database in 2019. *Nucleic Acids Research*,
1145 47(D1), D1179-D1185. <https://doi.org/10.1093/nar/gky974>
- 1146 Damodaran, S., & Parkin, K. L. (2017). *Fennema's food chemistry* (5th ed.). Boca Raton (USA): CRC
1147 Press.

- 1148 De León, G., Fröhlich, E., & Salar-Behzadi, S. (2021). Bitter taste *in silico*: A review on virtual ligand
1149 screening and characterization methods for TAS2R-bitterant interactions. *International*
1150 *Journal of Pharmaceutics*, 600, 120486. <https://doi.org/10.1016/j.ijpharm.2021.120486>
- 1151 De León, G., Fröhlich, E., Fink, E., Di Pizio, A., & Salar-Behzadi, S. (2022). Premexotac: Machine
1152 learning bitterants predictor for advancing pharmaceutical development. *International*
1153 *Journal of Pharmaceutics*, 628, 122263. <https://doi.org/10.1016/j.ijpharm.2022.122263>
- 1154 Deng, X., Lin, H., Ahmed, I., & Sui, J. (2021). Isolation and identification of the umami peptides
1155 from *Trachinotus ovatus* hydrolysate by consecutive chromatography and Nano-HPLC-
1156 MS/MS. *LWT-Food Science and Technology*, 141, 110887.
1157 <https://doi.org/10.1016/j.lwt.2021.110887>
- 1158 DeSimone, J. A., & Lyall, V. (2006). Taste receptors in the gastrointestinal tract III. Salty and sour
1159 taste: sensing of sodium and protons by the tongue. *American Journal of Physiology-*
1160 *Gastrointestinal and Liver Physiology*, 291(6), G1005-G1010.
1161 <https://doi.org/10.1152/ajpgi.00235.2006>
- 1162 Di Lorenzo, P. M., Chen, J.-Y., Rosen, A. M., & Roussin, A. T. (2009). Tastant. In M. D. Binder, N.
1163 Hirokawa & U. Windhorst (Eds.), *Encyclopedia of neuroscience*, (pp. 4014-4019). Berlin
1164 (Germany): Springer.
- 1165 Di Pizio, A., & Niv, M. Y. (2015). Promiscuity and selectivity of bitter molecules and their receptors.
1166 *Bioorganic & Medicinal Chemistry*, 23(14), 4082-4091.
1167 <https://doi.org/10.1016/j.bmc.2015.04.025>
- 1168 Doty, R. L., Bagla, R., Morgenson, M., & Mirza, N. (2001). NaCl thresholds: Relationship to anterior
1169 tongue locus, area of stimulation, and number of fungiform papillae. *Physiology & Behavior*,
1170 72(3), 373-378. [https://doi.org/10.1016/S0031-9384\(00\)00416-9](https://doi.org/10.1016/S0031-9384(00)00416-9)
- 1171 Drew, M. G. B., Wilden, G. R. H., Spillane, W. J., Walsh, R. M., Ryder, C. A., & Simmie, J. M.
1172 (1998). Quantitative structure-activity relationship studies of sulfamates RNHSO₃Na:
1173 Distinction between sweet, sweet-bitter, and bitter molecules. *Journal of Agricultural and*
1174 *Food Chemistry*, 46(8), 3016-3026. <https://doi.org/10.1021/jf980095c>
- 1175 Durant, J. L., Leland, B. A., Henry, D. R., & Nourse, J. G. (2002). Reoptimization of MDL keys for
1176 use in drug discovery. *Journal of Chemical Information and Computer Sciences*, 42(6), 1273-
1177 1280. <https://doi.org/10.1021/ci010132r>
- 1178 Dutta, A., Bereau, T., & Vilgis, T. A. (2022a). Identifying sequential residue patterns in bitter and
1179 umami peptides. *ACS Food Science & Technology*, 2(11), 1773-1780.
1180 <https://doi.org/10.1021/acsfoodscitech.2c00251>

- 1181 Dutta, P., Jain, D., Gupta, R., & Rai, B. (2022b). Classification of tastants: A deep learning based
1182 approach. *ChemRxiv*. <https://doi.org/10.26434/chemrxiv-2022-rs6x3>
- 1183 Freund, Y., & Schapire, R. E. (1997). A decision-theoretic generalization of on-line learning and an
1184 application to boosting. *Journal of Computer and System Sciences*, 55(1), 119-139.
1185 <https://doi.org/10.1006/jcss.1997.1504>
- 1186 Fritz, F., Preissner, R., & Banerjee, P. (2021). VirtualTaste: A web server for the prediction of
1187 organoleptic properties of chemical compounds. *Nucleic Acids Research*, 49(W1), W679-
1188 W684. <https://doi.org/10.1093/nar/gkab292>
- 1189 Gaulton, A., Bellis, L. J., Bento, A. P., Chambers, J., Davies, M., Hersey, A., Light, Y., McGlinchey,
1190 S., Michalovich, D., & Al-Lazikani, B. (2012). ChEMBL: A large-scale bioactivity database
1191 for drug discovery. *Nucleic Acids Research*, 40(D1), D1100-D1107.
1192 <https://doi.org/10.1093/nar/gkr777>
- 1193 Gilbertson, T. A., Fontenot, D. T., Liu, L., Zhang, H., & Monroe, W. T. (1997). Fatty acid modulation
1194 of K⁺ channels in taste receptor cells: Gustatory cues for dietary fat. *American Journal of*
1195 *Physiology-Cell Physiology*, 272(4), C1203-C1210.
1196 <https://doi.org/10.1152/ajpcell.1997.272.4.C1203>
- 1197 Goel, A., Gajula, K., Gupta, R., & Rai, B. (2021). In-silico screening of database for finding potential
1198 sweet molecules: A combined data and structure based modeling approach. *Food Chemistry*,
1199 343, 128538. <https://doi.org/10.1016/j.foodchem.2020.128538>
- 1200 Gramatica, P. (2007). Principles of QSAR models validation: Internal and external. *QSAR &*
1201 *Combinatorial Science*, 26(5), 694-701. <https://doi.org/10.1002/qsar.200610151>
- 1202 Gu, J., Gui, Y., Chen, L., Yuan, G., Lu, H.-Z., & Xu, X. (2013). Use of natural products as chemical
1203 library for drug discovery and network pharmacology. *PloS one*, 8(4), e62839.
1204 <https://doi.org/10.1371/journal.pone.0062839>
- 1205 Hand, D. J. (1997). *Construction and assessment of classification rules*. Chichester (UK): Wiley.
- 1206 Huang, H.-L., Charoenkwan, P., Kao, T.-F., Lee, H.-C., Chang, F.-L., Huang, W.-L., Ho, S.-J., Shu,
1207 L.-S., Chen, W.-L., & Ho, S.-Y. (2012). Prediction and analysis of protein solubility using a
1208 novel scoring card method with dipeptide composition. *BMC Bioinformatics*, 13(S17), S3.
1209 <https://doi.org/10.1186/1471-2105-13-S17-S3>
- 1210 Huang, W., Shen, Q., Su, X., Ji, M., Liu, X., Chen, Y., Lu, S., Zhuang, H., & Zhang, J. (2016).
1211 BitterX: A tool for understanding bitter taste in humans. *Scientific Reports*, 6, 23450.
1212 <https://doi.org/10.1038/srep23450>
- 1213 Kelly, D. P., Spillane, W. J., & Newell, J. (2005). Development of structure-taste relationships for
1214 monosubstituted phenylsulfamate sweeteners using classification and regression tree (CART)

1215 analysis. *Journal of Agricultural and Food Chemistry*, 53(17), 6750-6758.
1216 <https://doi.org/10.1021/jf0507137>

1217 Kier, L. B. (1980). Molecular structure influencing either a sweet or bitter taste among aldoximes.
1218 *Journal of Pharmaceutical Sciences*, 69(4), 416-419. <https://doi.org/10.1002/jps.2600690414>

1219 Kode srl. (2018). Dragon version 7. Software for molecular descriptor calculation, [http://chm.kode-](http://chm.kode-solutions.net/)
1220 [solutions.net/](http://chm.kode-solutions.net/)

1221 Kowalski, B., & Bender, C. (1972). *k*-Nearest Neighbor classification rule (pattern recognition)
1222 applied to nuclear magnetic resonance spectral interpretation. *Analytical Chemistry*, 44(8),
1223 1405-1411. <https://doi.org/10.1021/ac60316a008>

1224 Lavine, B. K., & Rayens, W. S. (2009). 3.27 - Classification: Basic Concepts. In S. Brown, R. Tauler
1225 & B. Walczak (Eds.), *Comprehensive Chemometrics (Second Edition)*, (pp. 567-573). Oxford,
1226 England: Elsevier. <https://doi.org/10.1016/B978-0-444-64165-6.01010-7>

1227 Lee, J., Song, S. B., Chung, Y. K., Jang, J. H., & Huh, J. (2022). BoostSweet: Learning molecular
1228 perceptual representations of sweeteners. *Food Chemistry*, 383, 132435.
1229 <https://doi.org/10.1016/j.foodchem.2022.132435>

1230 Ley, J., Reichelt, K., Obst, K., Krammer, G., & Engel, K. H. (2012). Important tastants and new
1231 developments. In H. Jeleń (Ed.), *Food flavors: Chemical, sensory and technological*
1232 *properties*, (pp. 19-33). Boca Raton (USA): CRC Press.

1233 Liang, L., Duan, W., Zhang, J., Huang, Y., Zhang, Y., & Sun, B. (2022a). Characterization and
1234 molecular docking study of taste peptides from chicken soup by sensory analysis combined
1235 with nano-LC-Q-TOF-MS/MS. *Food Chemistry*, 383, 132455.
1236 <https://doi.org/10.1016/j.foodchem.2022.132455>

1237 Liang, L., Zhou, C., Zhang, J., Huang, Y., Zhao, J., Sun, B., & Zhang, Y. (2022b). Characteristics of
1238 umami peptides identified from porcine bone soup and molecular docking to the taste receptor
1239 T1R1/T1R3. *Food Chemistry*, 387, 132870. <https://doi.org/10.1016/j.foodchem.2022.132870>

1240 Liu, Z., Zhu, Y., Wang, W., Zhou, X., Chen, G., & Liu, Y. (2020). Seven novel umami peptides from
1241 Takifugu rubripes and their taste characteristics. *Food Chemistry*, 330, 127204.
1242 <https://doi.org/10.1016/j.foodchem.2020.127204>

1243 Malavolta, M., Pallante, L., Mavkov, B., Stojceski, F., Grasso, G., Korfiati, A., Mavroudi, S.,
1244 Kalogeras, A., Alexakos, C., & Martos, V. (2022). A survey on computational taste predictors.
1245 *European Food Research and Technology*, 248, 2215-2235. [https://doi.org/10.1007/s00217-](https://doi.org/10.1007/s00217-022-04044-5)
1246 [022-04044-5](https://doi.org/10.1007/s00217-022-04044-5)

- 1247 Margulis, E., Dagan-Wiener, A., Ives, R. S., Jaffari, S., Siems, K., & Niv, M. Y. (2021). Intense
1248 bitterness of molecules: Machine learning for expediting drug discovery. *Computational and*
1249 *Structural Biotechnology Journal*, 19, 568-576. <https://doi.org/10.1016/j.csbj.2020.12.030>
- 1250 Margulis, E., Slavutsky, Y., Lang, T., Behrens, M., Benjamini, Y., & Niv, M. Y. (2022). BitterMatch:
1251 Recommendation systems for matching molecules with bitter taste receptors. *Journal of*
1252 *Cheminformatics*, 14(1), 45. <https://doi.org/10.1186/s13321-022-00612-9>
- 1253 Maroni, G., Pallante, L., Di Benedetto, G., Deriu, M. A., Piga, D., & Grasso, G. (2022). Informed
1254 classification of sweeteners/bitterants compounds via explainable machine learning. *Current*
1255 *Research in Food Science*, 5, 2270-2280. <https://doi.org/10.1016/j.crfs.2022.11.014>
- 1256 Martinez-Mayorga, K., & Medina-Franco, J. L. (2014). *Foodinformatics: Applications of chemical*
1257 *information to food chemistry*. Cham (Switzerland): Springer.
- 1258 Mathea, M., Klingspohn, W., & Baumann, K. (2016). Chemoinformatic classification methods and
1259 their applicability domain. *Molecular Informatics*, 35, 160-180.
1260 <https://doi.org/10.1002/minf.201501019>
- 1261 Matsunami, H., Montmayeur, J.-P., & Buck, L. B. (2000). A family of candidate taste receptors in
1262 human and mouse. *Nature*, 404, 601-604. <https://doi.org/10.1038/35007072>
- 1263 Mauri, A., & Bertola, M. (2022). Alvascience: A New Software Suite for the QSAR Workflow
1264 Applied to the Blood-Brain Barrier Permeability. *International Journal of Molecular*
1265 *Sciences*, 23(21), 12882. <https://doi.org/10.3390/ijms232112882>
- 1266 McLachlan, G. J. (1992). *Discriminant analysis and statistical pattern recognition*. New York
1267 (USA): Wiley.
- 1268 Minkiewicz, P., Dziuba, J., Iwaniak, A., Dziuba, M., & Darewicz, M. (2008). BIOPEP database and
1269 other programs for processing bioactive peptide sequences. *Journal of AOAC International*,
1270 91(4), 965-980. <https://doi.org/10.1093/jaoac/91.4.965>
- 1271 Miyashita, Y., Takahashi, Y., Takayama, C., Sumi, K., Nakatsuka, K., Ohkubo, T., Abe, H., & Sasaki,
1272 S.-i. (1986a). Structure-taste correlation of L-Aspartyl dipeptides using the SIMCA method.
1273 *Journal of Medicinal Chemistry*, 29(6), 906-912. <https://doi.org/10.1021/jm00156a006>
- 1274 Miyashita, Y., Takahashi, Y., Takayama, C., Ohkubo, T., Funatsu, K., & Sasaki, S.-i. (1986b).
1275 Computer-assisted structure/taste studies on sulfamates by pattern recognition methods.
1276 *Analytica Chimica Acta*, 184, 143-149. [https://doi.org/10.1016/S0003-2670\(00\)86477-6](https://doi.org/10.1016/S0003-2670(00)86477-6)
- 1277 Morgan, H. L. (1965). The generation of a unique machine description for chemical structures-a
1278 technique developed at chemical abstracts service. *Journal of Chemical Documentation*, 5(2),
1279 107-113. <https://doi.org/10.1021/c160017a018>

- 1280 Morini, G., Bassoli, A., & Borgonovo, G. (2011). Molecular modelling and models in the study of
1281 sweet and umami taste receptors. A review. *Flavour and Fragrance Journal*, 26(4), 254-259.
1282 <https://doi.org/10.1002/ffj.2054>
- 1283 Moriwaki, H., Tian, Y.-S., Kawashita, N., & Takagi, T. (2018). Mordred: A molecular descriptor
1284 calculator. *Journal of Cheminformatics*, 10, 4. <https://doi.org/10.1186/s13321-018-0258-y>
- 1285 O'Boyle, N. M., Morley, C., & Hutchison, G. R. (2008). Pybel: a Python wrapper for the OpenBabel
1286 cheminformatics toolkit. *Chemistry Central Journal*, 2, 5. <https://doi.org/10.1186/1752-153X-2-5>
- 1287
- 1288 Okuyama, T., Miyashita, Y., Kanaya, S., Katsumi, H., Sasaki, S.-i., & Randić, M. (1988). Computer
1289 assisted structure-taste studies on sulfamates by pattern recognition method using graph
1290 theoretical invariants. *Journal of Computational Chemistry*, 9(6), 636-646.
1291 <https://doi.org/10.1002/jcc.540090609>
- 1292 Oliveri, P. (2017). Class-modelling in food analytical chemistry: Development, sampling,
1293 optimisation and validation issues - A tutorial. *Analytica Chimica Acta*, 982, 9-19.
1294 <https://doi.org/10.1016/j.aca.2017.05.013>
- 1295 Pallante, L., Korfiati, A., Androutsos, L., Stojceski, F., Bompotas, A., Giannikos, I., Raftopoulos, C.,
1296 Malavolta, M., Grasso, G., Mavroudi, S., Kalogeras, A., Martos, V., Amoroso, D., Piga, D.,
1297 Theofilatos, K., & Deriu, M. A. (2022). Toward a general and interpretable umami taste
1298 predictor using a multi-objective machine learning approach. *Scientific Reports*, 12, 21735.
1299 <https://doi.org/10.1038/s41598-022-25935-3>
- 1300 Pieroni, A., Quave, C., Nebel, S., & Heinrich, M. (2002). Ethnopharmacy of the ethnic Albanians
1301 (Arbëreshë) of northern Basilicata, Italy. *Fitoterapia*, 73(3), 217-241.
1302 [https://doi.org/10.1016/S0367-326X\(02\)00063-1](https://doi.org/10.1016/S0367-326X(02)00063-1)
- 1303 Pieroni, A., Houlihan, L., Ansari, N., Hussain, B., & Aslam, S. (2007). Medicinal perceptions of
1304 vegetables traditionally consumed by South-Asian migrants living in Bradford, Northern
1305 England. *Journal of Ethnopharmacology*, 113(1), 100-110.
1306 <https://doi.org/10.1016/j.jep.2007.05.009>
- 1307 Rhyu, M.-R., Kim, Y., & Lyall, V. (2021). Interactions between Chemesthesis and Taste: Role of
1308 TRPA1 and TRPV1. *International Journal of Molecular Sciences*, 22(7), 3360.
1309 <https://doi.org/10.3390/ijms22073360>
- 1310 Richard, A. M., & Williams, C. R. (2002). Distributed structure-searchable toxicity (DSSTox) public
1311 database network: A proposal. *Mutation Research/Fundamental and Molecular Mechanisms
1312 of Mutagenesis*, 499(1), 27-52. [https://doi.org/10.1016/S0027-5107\(01\)00289-5](https://doi.org/10.1016/S0027-5107(01)00289-5)

- 1313 Rodgers, S., Glen, R. C., & Bender, A. (2006). Characterizing bitterness: Identification of key
1314 structural features and development of a classification model. *Journal of Chemical*
1315 *Information and Modeling*, 46(2), 569-576. <https://doi.org/10.1021/ci0504418>
- 1316 Rogers, D., & Hahn, M. (2010). Extended-connectivity fingerprints. *Journal of Chemical Information*
1317 *and Modeling*, 50(5), 742-754. <https://doi.org/10.1021/ci100050t>
- 1318 Rojas, C., Duchowicz, P. R., Pis Diez, R., & Tripaldi, P. (2016a). Applications of quantitative
1319 structure-relative sweetness relationships in food chemistry. In A. G. Mercader, P. R.
1320 Duchowicz & P. M. Sivakumar (Eds.), *Chemometrics applications and research: QSAR in*
1321 *medicinal chemistry*, (pp. 317-339). Boca Raton (USA): Apple Academic Press.
- 1322 Rojas, C., Tripaldi, P., & Duchowicz, P. R. (2016b). A new QSPR study on relative sweetness.
1323 *International Journal of Quantitative Structure-Property Relationships*, 1(1), 78-92.
1324 <https://doi.org/10.4018/IJQSPR.2016010104>
- 1325 Rojas, C., Ballabio, D., Consonni, V., Tripaldi, P., Mauri, A., & Todeschini, R. (2016c). Quantitative
1326 structure-activity relationships to predict sweet and non-sweet tastes. *Theoretical Chemistry*
1327 *Accounts*, 135, 66. <https://doi.org/10.1007/s00214-016-1812-1>
- 1328 Rojas, C., Todeschini, R., Ballabio, D., Mauri, A., Consonni, V., Tripaldi, P., & Grisoni, F. (2017).
1329 A QSTR-based expert system to predict sweetness of molecules. *Frontiers in Chemistry*, 5,
1330 53. <https://doi.org/10.3389/fchem.2017.00053>
- 1331 Rojas, C., Ballabio, D., Pacheco Sarmiento, K., Pacheco Jaramillo, E., Mendoza, M., & García, F.
1332 (2022). *ChemTastesDB*: A curated database of molecular tastants. *Food Chemistry:*
1333 *Molecular Sciences*, 4, 100090. <https://doi.org/10.1016/j.fochms.2022.100090>
- 1334 Roper, S. D. (2007). Signal transduction and information processing in mammalian taste buds.
1335 *Pflügers Archiv-European Journal of Physiology*, 454, 759-776.
1336 <https://doi.org/10.1007/s00424-007-0247-x>
- 1337 Ruddigkeit, L., & Reymond, J.-L. (2014). The chemical space of flavours. In K. Martinez-Mayorga
1338 & J. L. Medina-Franco (Eds.), *Foodinformatics: Applications of chemical information to food*
1339 *chemistry*, (pp. 83-96). Cham (Switzerland): Springer.
- 1340 Sahigara, F., Mansouri, K., Ballabio, D., Mauri, A., Consonni, V., & Todeschini, R. (2012).
1341 Comparison of different approaches to define the applicability domain of QSAR models.
1342 *Molecules*, 17(5), 4791-4810. <https://doi.org/10.3390/molecules17054791>
- 1343 Sayers, E. W., Beck, J., Bolton, E. E., Bourexis, D., Brister, J. R., Canese, K., Comeau, D. C., Funk,
1344 K., Kim, S., & Klimke, W. (2021). Database resources of the national center for biotechnology
1345 information. *Nucleic Acids Research*, 49(D1), D10-D17. <https://doi.org/10.1093/nar/gkaa892>

- 1346 Schieberle, P., & Hofmann, T. (2016). Mapping the combinatorial code of food flavors by means of
1347 molecular sensory science approach. In H. Jeleń (Ed.), *Food flavors: Chemical, sensory and*
1348 *technological properties*, (pp. 413-438). Boca Raton (USA): CRC Press.
- 1349 Schrödinger LLC. (2015). QikProp, New York, NY.
- 1350 Schrödinger LLC. (2017). Canvas, New York, NY.
- 1351 Shiyan, R., Liping, S., Xiaodong, S., Jinlun, H., & Yongliang, Z. (2021). Novel umami peptides from
1352 tilapia lower jaw and molecular docking to the taste receptor T1R1/T1R3. *Food Chemistry*,
1353 *362*, 130249. <https://doi.org/10.1016/j.foodchem.2021.130249>
- 1354 Spillane, W. J., & McGlinchey, G. (1981). Structure-activity studies on sulfamate sweeteners II:
1355 Semiquantitative structure-taste relationship for sulfamate (RNHSO₃⁻) sweeteners-The role
1356 of R. *Journal of Pharmaceutical Sciences*, *70*(8), 933-935.
1357 <https://doi.org/10.1002/jps.2600700826>
- 1358 Spillane, W. J., McGlinchey, G., Muirheartaigh, I. Ó., & Benson, G. A. (1983). Structure-activity
1359 studies on sulfamate sweeteners III: Structure-taste relationships for heterosulfamates. *Journal*
1360 *of Pharmaceutical Sciences*, *72*(8), 852-856. <https://doi.org/10.1002/jps.2600720804>
- 1361 Spillane, W. J., & Sheahan, M. B. (1989). Semi-quantitative and quantitative structure-taste
1362 relationships for carbo and hetero-sulphamate (RNHSO₃⁻) sweeteners. *Journal of the*
1363 *Chemical Society, Perkin Transactions 2*(7), 741-746. <https://doi.org/10.1039/P29890000741>
- 1364 Spillane, W. J., Sheahan, M. B., & Ryder, C. A. (1993). Synthesis and taste properties of sodium
1365 disubstituted phenylsulfamates. Structure-taste relationships for sweet and bitter/sweet
1366 sulfamates. *Food Chemistry*, *47*(4), 363-369. [https://doi.org/10.1016/0308-8146\(93\)90178-I](https://doi.org/10.1016/0308-8146(93)90178-I)
- 1367 Spillane, W. J., Ryder, C. A., Walsh, M. R., Curran, P. J., Concagh, D. G., & Wall, S. N. (1996).
1368 Sulfamate sweeteners. *Food Chemistry*, *56*(3), 255-261. [https://doi.org/10.1016/0308-](https://doi.org/10.1016/0308-8146(96)00022-2)
1369 [8146\(96\)00022-2](https://doi.org/10.1016/0308-8146(96)00022-2)
- 1370 Spillane, W. J., Ryder, C. A., Curran, P. J., Wall, S. N., Kelly, L. M., Feeney, B. G., & Newell, J.
1371 (2000). Development of structure-taste relationships for sweet and non-sweet
1372 heterosulfamates. *Journal of the Chemical Society, Perkin Transactions 2*, *2*, 1369-1374.
1373 <https://doi.org/10.1039/B002482L>
- 1374 Spillane, W. J., Feeney, B. G., & Coyle, C. M. (2002). Further studies on the synthesis and tastes of
1375 monosubstituted benzenesulfamates. A semi-quantitative structure-taste relationship for the
1376 meta-compounds. *Food Chemistry*, *79*(1), 15-22. [https://doi.org/10.1016/S0308-](https://doi.org/10.1016/S0308-8146(02)00169-3)
1377 [8146\(02\)00169-3](https://doi.org/10.1016/S0308-8146(02)00169-3)
- 1378 Spillane, W. J., Kelly, L. M., Feeney, B. G., Drew, M. G., & Hattotuwigama, C. K. (2003). Synthesis
1379 of heterosulfamates. Search for structure-taste relationships. *Arkivoc*, *VII*, 297-309.

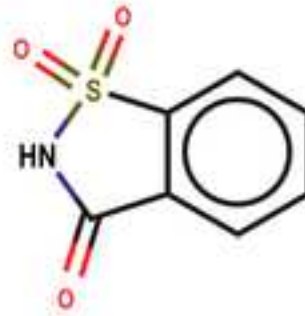
- 1380 Spillane, W. J., Kelly, D. P., Curran, P. J., & Feeney, B. G. (2006). Structure-taste relationships for
1381 disubstituted phenylsulfamate tastants using classification and regression tree (CART)
1382 analysis. *Journal of Agricultural and Food Chemistry*, 54(16), 5996-6004.
1383 <https://doi.org/10.1021/jf0606656>
- 1384 Spillane, W. J., Coyle, C. M., Feeney, B. G., & Thompson, E. F. (2009). Development of structure-
1385 taste relationships for thiazolyl-, benzothiazolyl-, and thiadiazolylsulfamates. *Journal of*
1386 *Agricultural and Food Chemistry*, 57(12), 5486-5493. <https://doi.org/10.1021/jf9002472>
- 1387 Suárez-Estrella, D., Borgonovo, G., Buratti, S., Ferranti, P., Accardo, F., Pagani, M. A., & Marti, A.
1388 (2021). Sprouting of quinoa (*Chenopodium quinoa* Willd.): Effect on saponin content and
1389 relation to the taste and astringency assessed by electronic tongue. *LWT-Food Science and*
1390 *Technology*, 144, 111234. <https://doi.org/10.1016/j.lwt.2021.111234>
- 1391 Suess, B., Festrings, D., & Hofmann, T. (2015). Umami compounds and taste enhancers. In J. K.
1392 Parker, J. S. Elmore & L. Methven (Eds.), *Flavour development, analysis and perception in*
1393 *food and beverages*, (pp. 331-351). Cambridge (UK): Woodhead Publishing.
- 1394 Takahashi, Y., Miyashita, Y., Tanaka, Y., Abe, H., & Sasaki, S. (1982). A consideration for structure-
1395 taste correlations of perillartines using pattern-recognition techniques. *Journal of Medicinal*
1396 *Chemistry*, 25(10), 1245-1248. <https://doi.org/10.1021/jm00352a030>
- 1397 Takahashi, Y., Abe, H., Miyashita, Y., Tanaka, Y., Hayasaka, H., & Sasaki, S. I. (1984).
1398 Discriminative structural analysis using pattern recognition techniques in the structure-taste
1399 problem of perillartines. *Journal of Pharmaceutical Sciences*, 73(6), 737-741.
1400 <https://doi.org/10.1002/jps.2600730608>
- 1401 Todeschini, R., & Consonni, V. (2009). *Molecular descriptors for chemoinformatics (2 volumes)*
1402 (Second ed.). Weinheim (Germany): Wiley-VCH.
- 1403 Todeschini, R., Ballabio, D., Cassotti, M., & Consonni, V. (2015a). N3 and BNN: Two new similarity
1404 based classification methods in comparison with other classifiers. *Journal of Chemical*
1405 *Information and Modeling*, 55(11), 2365-2374. <https://doi.org/10.1021/acs.jcim.5b00326>
- 1406 Todeschini, R., Ballabio, D., & Consonni, V. (2015b). Distances and other dissimilarity measures in
1407 chemometrics. In R. A. Meyers (Ed.), *Encyclopedia of analytical chemistry: Applications,*
1408 *theory and instrumentation*, (pp. 1-34): JohnWiley & Sons, Ltd.
- 1409 Tuwani, R., Wadhwa, S., & Bagler, G. (2019). BitterSweet: Building machine learning models for
1410 predicting the bitter and sweet taste of small molecules. *Scientific Reports*, 9, 7155.
1411 <https://doi.org/10.1038/s41598-019-43664-y>
- 1412 van der Maaten, L., & Hinton, G. (2008). Visualizing data using t-SNE. *Journal of Machine Learning*
1413 *Research*, 9, 2579-2605.

- 1414 Vapnik, V. (1998). The support vector method of function estimation. In J. A. K. Suykens & J.
1415 Vandewalle (Eds.), *Nonlinear modeling: Advanced black-box techniques*, (pp. 55-85). Boston
1416 (USA): Kluwer Academic Publishers.
- 1417 Walters, D. E. (2006). Analysing and predicting properties of sweet-tasting compounds. In W. J.
1418 Spillane (Ed.), *Optimising sweet taste in foods*, (pp. 283-291). Boca Raton (USA): CRC Press.
- 1419 Wiener, A., Shudler, M., Levit, A., & Niv, M. Y. (2012). BitterDB: A database of bitter compounds.
1420 *Nucleic Acids Research*, 40(D1), D413-D419. <https://doi.org/10.1093/nar/gkr755>
- 1421 Wold, S., & Eriksson, L. (1995). Statistical validation of QSAR results. Validation tools. In H. van
1422 de Waterbeemd (Ed.), *Chemometric methods in molecular design*, (pp. 309-318). Weinheim
1423 (Germany): VCH Publishers.
- 1424 Wong, D. W. (2018). *Mechanism and theory in food chemistry* (2nd ed.). Cham (Switzerland):
1425 Springer.
- 1426 Xiu, H., Liu, Y., Yang, H., Ren, H., Luo, B., Wang, Z., Shao, H., Wang, F., Zhang, J., & Wang, Y.
1427 (2022). Identification of novel umami molecules via QSAR models and molecular docking.
1428 *Food & Function*, 13, 7529-7539. <https://doi.org/10.1039/D2FO00544A>
- 1429 Yang, Z.-F., Xiao, R., Xiong, G.-L., Lin, Q.-L., Liang, Y., Zeng, W.-B., Dong, J., & Cao, D.-s. (2022).
1430 A novel multi-layer prediction approach for sweetness evaluation based on systematic
1431 machine learning modeling. *Food Chemistry*, 372, 131249.
1432 <https://doi.org/10.1016/j.foodchem.2021.131249>
- 1433 Yu, Z., Jiang, H., Guo, R., Yang, B., You, G., Zhao, M., & Liu, X. (2018). Taste, umami-enhance
1434 effect and amino acid sequence of peptides separated from silkworm pupa hydrolysate. *Food*
1435 *Research International*, 108, 144-150. <https://doi.org/10.1016/j.foodres.2018.02.047>
- 1436 Zheng, S., Jiang, M., Zhao, C., Zhu, R., Hu, Z., Xu, Y., & Lin, F. (2018). e-Bitter: Bitterant prediction
1437 by the consensus voting from the machine-learning methods. *Frontiers in Chemistry*, 6, 82.
1438 <https://doi.org/10.3389/fchem.2018.00082>
- 1439 Zheng, S., Chang, W., Xu, W., Xu, Y., & Lin, F. (2019). e-Sweet: A machine-learning based platform
1440 for the prediction of sweetener and its relative sweetness. *Frontiers in Chemistry*, 7, 35.
1441 <https://doi.org/10.3389/fchem.2019.00035>
- 1442

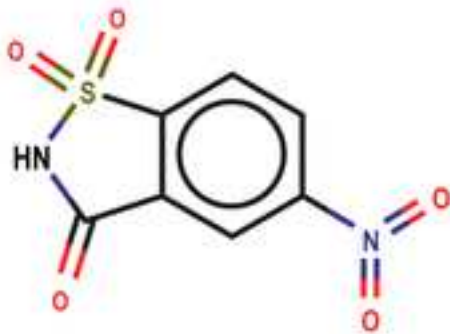
Figure 1. Taste changes of saccharin when introducing the nitro and amino molecular fragments in diverse position of the chemical scaffold.

Figure 2. Representation of classification boundaries (black lines) between sweet (blue) and bitter (red) chemicals in the space of the first two t-SNE dimensions (latent variables for PLSDA). The results are presented for different classifiers.

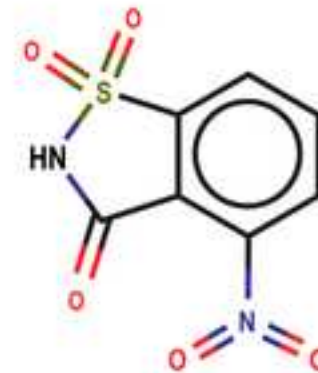
Figure 3. Number of molecules (expressed as log₁₀) used for the calculation of models for taste prediction vs publication year.



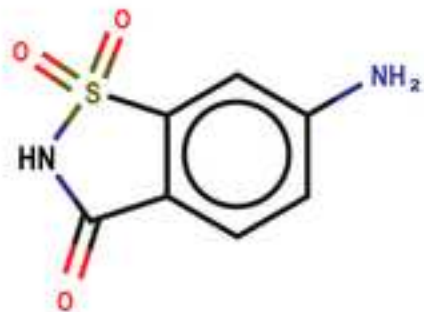
Saccharin (sweet)



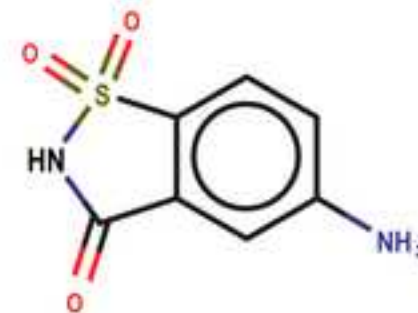
5-Nitrosaccharin (Bitter)



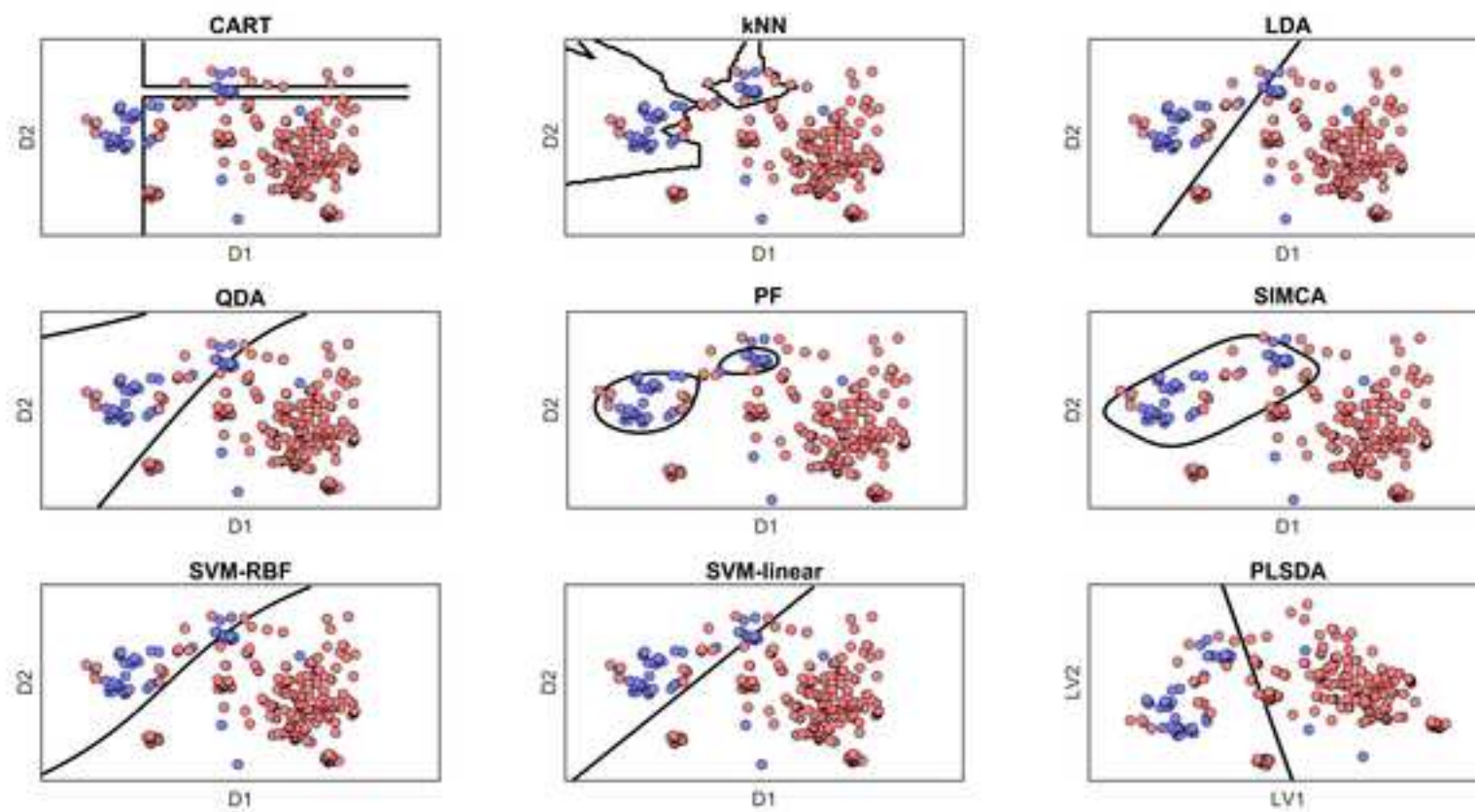
p-Nitrosaccharin (Sweet/Bitter)



6-Aminosaccharin (Sweet/Tasteless)



5-Aminosaccharin (Tasteless)



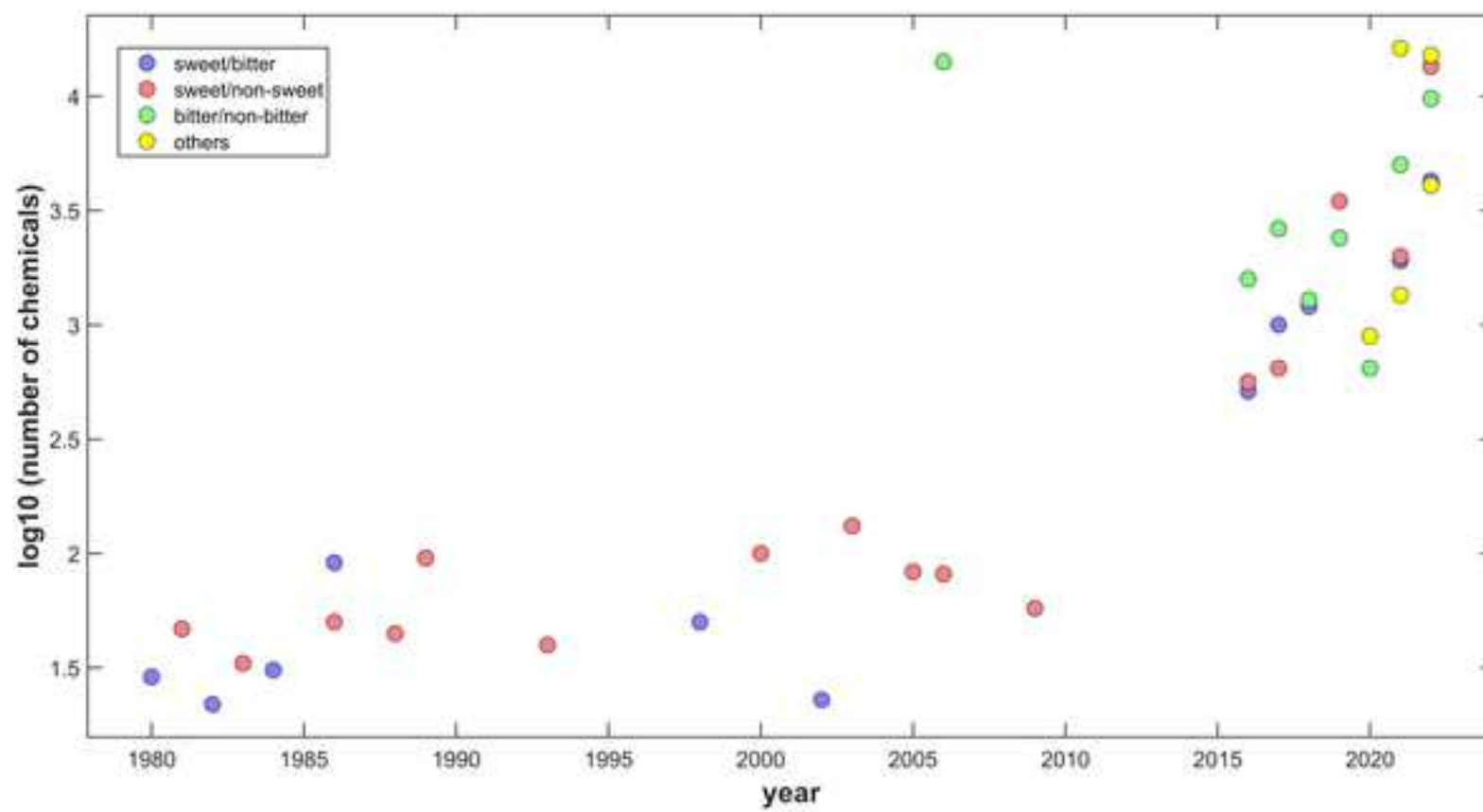


Table 1. Classification-based machine learning models for the discrimination between sweet and bitter tastants. d is the number of descriptors, n is the number of molecules.

Table 2. Classification-based machine learning models for the discrimination between sweet and non-sweet tastants. d is the number of descriptors, n is the number of molecules.

Table 3. Classification-based machine learning models for the prediction of bitterness. d is the number of descriptors, n is the number of molecules.

Table 1

reference	URL	Model name	Classifier	d	training				test			
					n	NER	AUC	F-score	n	NER	AUC	F-score
(Kier, 1980)	--	--	LDA	2	20	0.850	--	--	9	0.875	--	--
(Takahashi <i>et al.</i> , 1982)	--	--	k NN	3	22	0.909	--	--	--	--	--	--
			LDA			1	--	--	--	--	--	
(Takahashi <i>et al.</i> , 1984)	--	--	LDA	3	22	1	--	--	9	0.775	--	--
				2		0.955	--	--		0.775	--	--
(Miyashita <i>et al.</i> , 1986a)	--	--	SIMCA	5	91	0.840			--	--	--	--
(Drew <i>et al.</i> , 1998)	--	--	DA	11	50	1	--	--	--	--	--	--
(Spillane <i>et al.</i> , 2002)	--	--	Biplot	2	23	0.862	--	--	--	--	--	--
			LDA	4		0.850	--	--	--	--	--	
			QDA	4		0.900	--	--	--	--	--	
(Rojas <i>et al.</i> , 2016c)	--	--	k NN	4	356	0.864	--	--	152	0.789	--	--
(Chéron <i>et al.</i> , 2017)	http://sebfiorucci.free.fr/SweetenersDB/	--	RF	5 ^a	796	0.997	--	--	200	0.914	--	--
(Banerjee & Preissner, 2018)	--	BitterSweetForest	RF	2,048	961	0.950 ^b	0.980	0.940	241	0.967 ^b	0.980	0.920
(Goel <i>et al.</i> , 2021)	--	--	RF	8	1,537	0.908	--	--	385	0.855	--	--
(Bo <i>et al.</i> , 2022)	--	BitterSweetMLP-Fingerprint	MLP	17	1,637	0.870	0.950	--	409	0.880	0.950	--
(Maroni <i>et al.</i> , 2022)	https://github.com/gabribg88/VirtuousSweetBitter https://virtuoussh2020.com/	--	GBM	9	2,195	0.893	0.950	0.883	--	--	--	--

^a number of descriptors for the tree depth; ^b calculated as Accuracy (ACC)

Table 2

reference	URL	Model name	Classifier	d	training				test			
					n	NER	AUC	F-score	n	NER	AUC	F-score
(Spillane & McGlinchey, 1981)	--	--	DA-plot	2	47	0.957 ^b	--	--	--	--	--	--
(Spillane <i>et al.</i> , 1983)	--	--	LDA	3	33	0.807	--	--	--	--	--	--
(Miyashita <i>et al.</i> , 1986b)	--	--	SIMCA	4	50	0.798	--	--	--	--	--	--
(Okuyama <i>et al.</i> , 1988)	--	--	SIMCA	1 ^a	25	0.868	--	--	--	--	--	--
					20	0.808	--	--	--	--	--	--
(Spillane & Sheahan, 1989)	--	--	DA-plot	2	17	0.824 ^b	--	--	--	--	--	--
			LDA	3	23	0.642	--	--	--	--	--	--
					56	0.773	--	--	--	--	--	--
(Spillane <i>et al.</i> , 1993)	--	--	DA-plot	2	40	--	--	--	--	--	--	
(Spillane <i>et al.</i> , 2000)	--	--	QDA	4	101	0.801	--	--	--	--	--	--
(Spillane <i>et al.</i> , 2003)	--	--	CART	4	132	0.815	--	--	--	--	--	--
(Kelly <i>et al.</i> , 2005)	--	--	CART	6	75	0.768	--	--	8	0.750	--	--
(Spillane <i>et al.</i> , 2006)	--	--	CART	7	70	0.807	--	--	12	0.909	--	--
(Spillane <i>et al.</i> , 2009)	--	--	CART	6	48	0.950	--	--	10	0.625	--	--
(Rojas <i>et al.</i> , 2016c)	--	--	k NN	9	396	0.838	--	--	170	0.752	--	--
(Rojas <i>et al.</i> , 2017)	--	--	Expert System	--	488	0.892	--	--	161	0.848	--	--
(Zheng <i>et al.</i> , 2019)	https://www.dropbox.com/sh/1fmlv7nf6wofgcp/AADBjzFbbiNRJUP0806wSyna?dl=0	e-Sweet	Consensus	--	883	0.870	--	0.850	221	0.900	--	0.878
(Tuwani <i>et al.</i> , 2019)	https://github.com/cosylabiiii/bittersweet/ https://cosylab.iiitd.edu.in/bittersweet/	BitterSweet	AdaBoost	--	2,205	0.856	0.918	0.858	161	0.834	0.883	0.856
(Fritz <i>et al.</i> , 2021)	http://virtualtaste.charite.de/VirtualTaste/	VirtualSweet	RF	--	1,608	0.970	0.990	0.870	403	0.893	0.951	0.888
(Yang <i>et al.</i> , 2022)	--	--	RF	241	959	0.873	0.958	--	241	0.920	0.971	--

	https://github.com/ifyoungnet/ChemSweet		XGBoost	95	366	0.905	0.956	--	92	0.926	0.974	--
				105	1,327	0.834	0.926	--	333	0.841	0.920	--
				124	2,104	0.870	0.947	--	527	0.867	0.947	--
				102	394	0.893	0.937	--	100	0.876	0.956	--
				122	2,091	0.875	0.949	--	522	0.889	0.961	--
(Bo <i>et al.</i> , 2022)	--	SweetMLP-Fingerprint	MLP	--	1,776	0.860	0.930	--	444	0.900	0.940	--
		SweetCNN	CNN			0.860	0.900	--		0.850	0.900	--
(Lee <i>et al.</i> , 2022)	--	BoostSweet	Soft-vote consensus	--	1,832	--	--	--	459	0.899	0.961	0.907

^a number of principal components (PCs); ^b calculated as Accuracy (ACC)

Table 3

reference	URL	Model name	Classifier	d	training				test			
					n	NER	AUC	F-score	n	NER	AUC	F-score
(Rodgers <i>et al.</i> , 2006)	--	--	Naïve Bayes	10	14,179	0.805	--	--	--	--	--	--
(Huang <i>et al.</i> , 2016)	http://mdl.shsmu.edu.cn/BitterX	BitterX	SVM	46	862	0.879 ^b	--	--	216	0.915 ^b	0.950	--
				35	416	0.767 ^b	--	--	104	0.798 ^b	0.823	--
(Dagan-Wiener <i>et al.</i> , 2017)	https://github.com/Niv-Lab/BitterPredict1	BitterPredict	AdaBoost	16 ^a	1,827	0.921	--	--	781	0.812	--	--
(Zheng <i>et al.</i> , 2018)	https://www.dropbox.com/sh/3sebvza3qzmazda/AADgpCRXJtHAJzS8DK_P-q0ka?dl=0	e-Bitter	Consensus	--	1,040	--	--	--	259	0.929 ^b	--	0.936
(Tuwani <i>et al.</i> , 2019)	https://github.com/cosylabiit/bittersweet/ https://cosylab.iiitd.edu.in/bittersweet/	BitterSweet	RF	--	2,257	0.754	0.852	0.698	154	0.819	0.880	0.838

(Charoenkwan <i>et al.</i> , 2020a)	http://camt.pythonanywhere.com/	iBitter-SCM	SCM	--	512	0.871 ^b			128	0.844 ^b		
(Margulis <i>et al.</i> , 2021)	--	BitterIntense	XGBoost	8	616	0.870 ^b	--	0.820	105	0.790	--	0.700
(Charoenkwan <i>et al.</i> , 2021a)	http://pmlab.pythonanywhere.com/BERT4Bitter	BERT4Bitter	BERT	--	512	0.861 ^b	0.915	--	128	0.922 ^b	0.964	--
(Fritz <i>et al.</i> , 2021)	http://virtualtaste.charite.de/VirtualTaste/	VirtualBitter	RF	--	1,289	0.960	0.975	0.946	323	0.898	0.956	0.882
(Charoenkwan <i>et al.</i> , 2021b)	http://camt.pythonanywhere.com/iBitter-Fuse	iBitter-Fuse	SVM	36	512	0.918 ^b	0.937	--	128	0.930 ^b	0.933	--
(Bai <i>et al.</i> , 2021)	--	CBDPS	XGBoost	--	1,296	0.882 ^b	--	0.881	112	--	--	--
(Bo <i>et al.</i> , 2022)	--	BitterMLP-Descriptor	MLP	15	1,787	0.830	0.920	--	446	0.820	0.940	--
		BitterCNN	CNN	--		0.770	0.870	--		0.790	0.880	--
(Margulis <i>et al.</i> , 2022)	https://github.com/YuliSI/BitterMatch	BitterMatch	XGBoost	20	3,601	0.759 ^c	--	--	900	--	--	--
					242	0.699 ^c	--	--	61	--	--	--
(De León <i>et al.</i> , 2022)	--	Premexotac	SVM	512	2,272	0.836 ^b	--	--	568	0.870 ^b	--	--
			AdaBoost	18		0.842 ^b	--	--		0.847 ^b	--	--

^a descriptors with the most significant contribution; ^b calculated as Accuracy (ACC), ^c reported as recall-precision

